Estuarine, Coastal and Shelf Science (2000) **50,** 467–488
doi:10.1006/ecss.2000.0593, available online at http://www.idealibrary.com on IDEAL®

What Determines Seasonal and Interannual Variability of Phytoplankton and Zooplankton in Strongly Estuarine Systems?
Application to the semi-enclosed estuary of Strait of Georgia and Juan de Fuca Strait

M. Li, A. Gargett and K. Denman

Institute of Ocean Sciences, P.O. Box 6000, Sidney, B.C. V8L 4B2, Canada

Received 3 February 1999 and accepted in revised form 3 January 2000

A coupled biological–physical box model is developed to investigate the seasonal and interannual variability of marine plankton in strongly estuarine systems such as the semi-enclosed estuary of the Strait of Georgia and Juan de Fuca Strait on the west coast of Canada. The estuarine circulation not only supplies nutrients to the euphotic layer but also transports plankton between the straits, causing an asymmetrical distribution of plankton biomass in the estuary. A specific set of biological parameters can be chosen so that the model predicts a large spring bloom and nutrient limitation in the Strait of Georgia but high nutrient levels and no spring bloom in the Juan de Fuca Strait, in agreement with observations. However, as the plankton growth and mortality rate parameters are varied over a realistic range, the plankton also exhibit two other ecosystem behaviours: one with a large spring bloom in the Juan de Fuca Strait and one with a low zooplankton stock in the Strait of Georgia.

To determine possible causes for observed interannual variability of the planktonic ecosystem, we have run the coupled biophysical model with stochastic variation of the Fraser River runoff and the shelf salinity. The plankton populations are found to be insensitive to the interannual variability in the estuarine circulation. It is suggested that marine phytoplankton and zooplankton might respond more significantly to climate variability (or change) through changes in their biological rate parameters.

Keywords: planktonic ecosystem; ecosystem; estuarine circulation; Canada west coast

Introduction

In the classic Sverdrup (1953) model, the seasonal development of marine phytoplankton is closely linked to the seasonal cycle of ocean mixed layer depth. Deep convective mixing during the winter replenishes the mixed layer with nutrients. As the light level increases and the mixed layer shallows in the spring, the phytoplankton grow faster, thus leading to a spring bloom in phytoplankton biomass. Nutrient limitation and/or zooplankton grazing subsequently reduce the phytoplankton standing stock. This one-dimensional (vertical) model has been a foundation for our understanding of marine ecosystems. Here we investigate seasonal to annual variation in a strongly estuarine system in which the estuarine circulation is the main mechanism delivering the nutrients and in which salinity determines the water column stratification. The objective is to identify which factors affect the seasonal and interannual variability of marine plankton residing in such a system.

The Strait of Georgia and Juan de Fuca Strait form a semi-enclosed estuary situated between Vancouver Island and the mainland coasts of British Columbia and Washington State (Figure 1). There is, on average, a two-layer exchange flow in the estuary (Thomson, 1981): the surface layer flows seaward, carrying fresh water from the rivers (primarily from the East River), and a subsurface layer flows landward, carrying saline and nutrient-rich water from the Pacific Ocean. Winds, tidal currents and mixing in narrow and shallow passages modulate this average circulation pattern.

The estuarine circulation creates a vigorous exchange of nutrients and plankton in the Georgia–Fuca Estuary (Mackas & Harrison, 1997). The deep return inflow which enters the lower layer of Juan de Fuca Strait imports nutrients from the Pacific Ocean. Some of the nutrients are brought up to the surface layer by tidal mixing in Haro Strait and then exported to Juan de Fuca Strait by the estuarine outflow, while the remaining nutrients flow at depth into the Strait of Georgia and are subsequently upwelled into the sunlit surface layer where they are available for biological utilization. Observations (Harrison *et al.*, 1983) show that a spring bloom develops in the Strait of Georgia

0272–7714/00/040467+22 $35.00/0

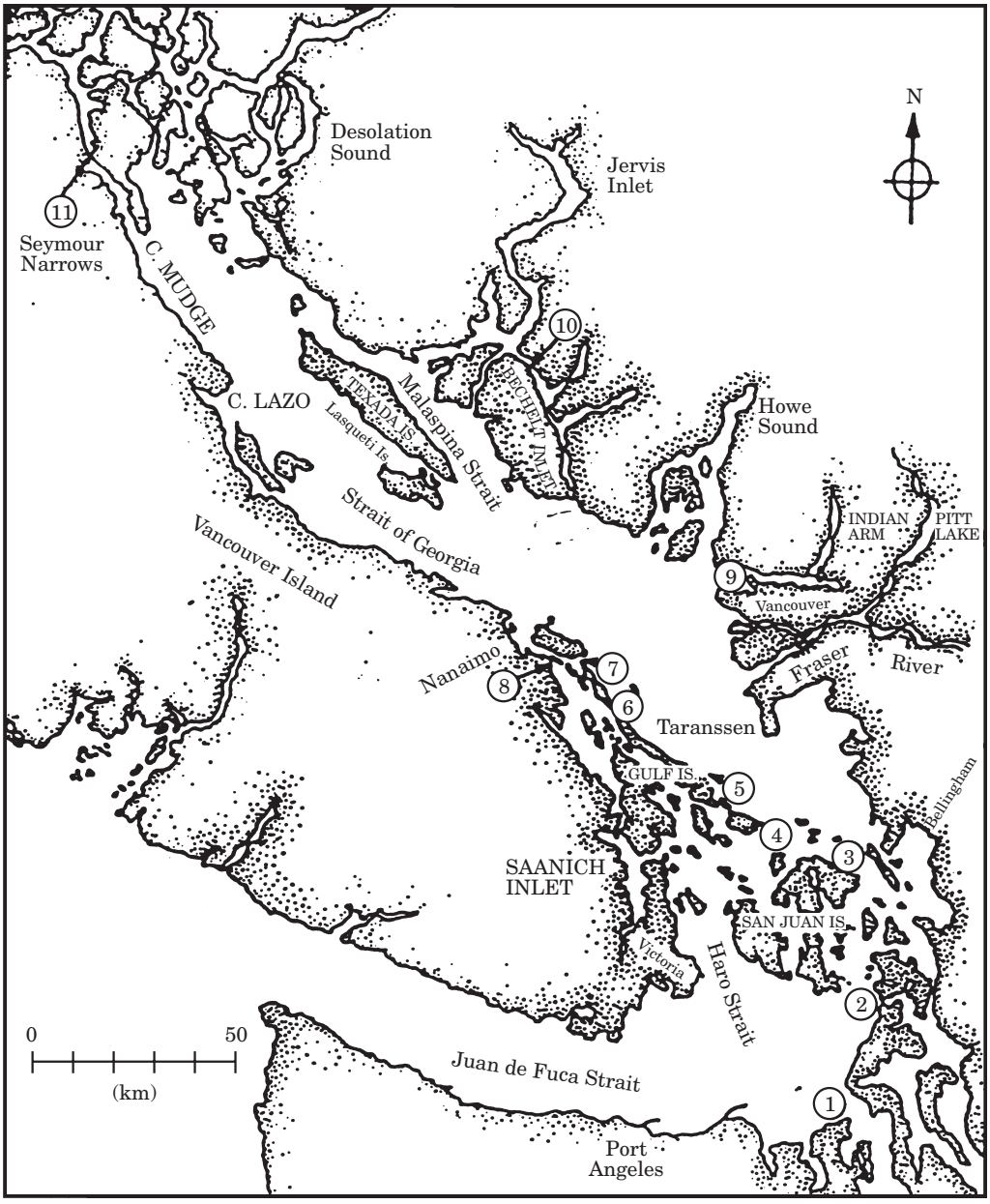

FIGURE 1. A map of the Strait of Georgia and Juan de Fuca Strait. The two basins are connected through the narrow channel of Haro Strait where tidal mixing is vigorous. Fresh water from the Fraser River is released into the Strait of Georgia, driving a two-layer estuarine circulation. The Puget Sound drainage basin (not shown) is connected to Juan de Fuca Strait through channels labelled 1.

in early March, which then leads to an increase in the zooplankton population and nutrient limitation during summer. Although there are always nutrients available in Juan de Fuca Strait, no significant spring bloom was observed (Mackas & Harrison, 1997). In this paper we investigate how the estuarine circulation affects the seasonal development of plankton populations in different parts of the estuarine system.

This work is also motivated by the apparent correlation that has been found between interdecadal variability in climate indices (e.g. Aleutian Low Pressure Index and Fraser River runoff) and fish stock fluctuations in the Strait of Georgia (Beamish *et al.*, 1997, 1995; Beamish & Bouillon, 1993). In order to understand how the oceanic physical environment affects fishery production at high trophic levels, we need first to understand how the physical environment affects the production of lower trophic level plankton because zooplankton are a major food source for juvenile fishes (e.g. Healey, 1980). Because of the

complexity of the marine foodweb system and lack of long-term biological observations, a coupled biological–physical model can be a useful tool for exploring possible links between the interannual variability in the marine physical system and year to year fluctuations in fish stocks.

Li *et al.* (1999) recently developed a box model for the estuarine circulation in the Georgia–Fuca Estuary. This model is now coupled with a foodweb model that includes nutrients, phytoplankton and zooplankton components. Because of its relatively modest demand on computer resources, the coupled model can be run repeatedly over climate time scales, allowing us to explore the sensitivity of marine ecosystem response to changes in various biological parameters. The box model has shown that estuarine circulation responds rapidly to interannual changes of Fraser River runoff (Li *et al.*, 1999): how does the planktonic ecosystem respond to the interannual variability in runoff? This and other questions shall be addressed in this paper.

This paper is arranged as follows. In the next section, the coupled biological–physical model is formulated for the Georgia–Fuca Estuary. This model differs from models used for open-ocean ecosystems where only vertical processes are usually considered (e.g. Evans & Parslow, 1985; Fasham *et al.*, 1990). In the following section we present model predictions for a typical seasonal cycle in the planktonic ecosystem, followed by a discussion on the role of the estuarine circulation in plankton production. Next, we examine the model sensitivity to interannual variability in the estuarine circulation, and then examine the model sensitivity to variations in biological parameters. In light of the coupled model results, we then discuss possible mechanisms which may link ocean climate variability with plankton ecosystem change in the Georgia–Fuca Estuary.

Model formulation

In the box model developed for the Strait of Georgia and Juan de Fuca Strait (Li *et al.*, 1999; see Appendix for a brief model description), the estuarine circulation transports not only salt but also nutrients, which may be utilized in biological production. This model of estuarine circulation can now be coupled with a biological model that has nutrients (N), phytoplankton (P) and zooplankton (Z) compartments. The concentration equations for the biological variables are given by

$$\frac{dP}{dt} = rP\min\left(\frac{N}{K_s+N}, \frac{I}{i_b+I}\right) - r_m\frac{P^2Z}{K_p^2+P^2} - p_mP, \quad (1)$$

$$\frac{dZ}{dt} = g_a r_m \frac{P^2Z}{K_p^2+P^2} - z_mZ, \quad (2)$$

$$\frac{dN}{dt} = -rP\min\left(\frac{N}{K_s+N}, \frac{I}{i_b+I}\right). \quad (3)$$

Here phytoplankton growth is either nutrient limited or light limited with a maximum growth rate r. The photosynthetically available radiation (PAR) is denoted by I. Both nutrient uptake and light utilization are described by Michaelis–Menton equations in which K_s is the half saturation constant for nutrient uptake and i_b is the half saturation constant for light utilization. The grazing of phytoplankton by zooplankton is represented by a Holling type III function where r_m is the maximum grazing rate and K_p the half-saturation constant. Only a fraction of ingested phytoplankton is assimilated into zooplankton biomass: the zooplankton grazing efficiency is denoted by g_a. Phytoplankton and zooplankton are assumed to have a mortality proportional to their population size: p_m is the mortality rate of phytoplankton and z_m is the mortality rate of zooplankton. Losses from unassimilated grazing and phytoplankton and zooplankton mortality are not recycled.

Phytoplankton and nutrients behave like passive scalars: they are transported between the boxes by horizontal advection and vertical mixing. It is assumed that photosynthesis occurs only in the surface boxes and phytoplankton do not grow once submerged into the deep boxes. Zooplankton are assumed to have vertical motility sufficient to remain in the euphotic upper boxes (e.g. as in the model of Evans & Parslow, 1985), although they can be advected horizontally between the upper boxes by the estuarine circulation. This treatment does not consider the life history of seasonal vertical migration of dominant copepod species such as *Neocalanus plumchrus* (Harrison *et al.*, 1983) not the diel migration undertaken by some species. Writing the concentration equations for each of the six boxes (cf. Appendix and Figure 2) gives the following set:

$$V_{gu}\frac{dP_{gu}}{dt} = Q_g(P_{gl}-P_{gu}) + \omega_g A_g(P_{gl}-P_{gu}) + rP_{gu}\min\left(\frac{N_{gu}}{K_s+N_{gu}}, \frac{I}{i_b+I}\right)V_{gu} - r_m\frac{P_{gu}{}^2Z_{gu}}{K_p^2+P_{gu}{}^2}V_{gu} - p_mP_{gu}V_{gu}, \quad (4)$$

$$V_{gu}\frac{dZ_{gu}}{dt} = -Q_gZ_{gu} + g_a r_m\frac{P_{gu}{}^2Z_{gu}}{K_p^2+P_{gu}{}^2}V_{gu} - z_mZ_{gu}V_{gu}, \quad (5)$$

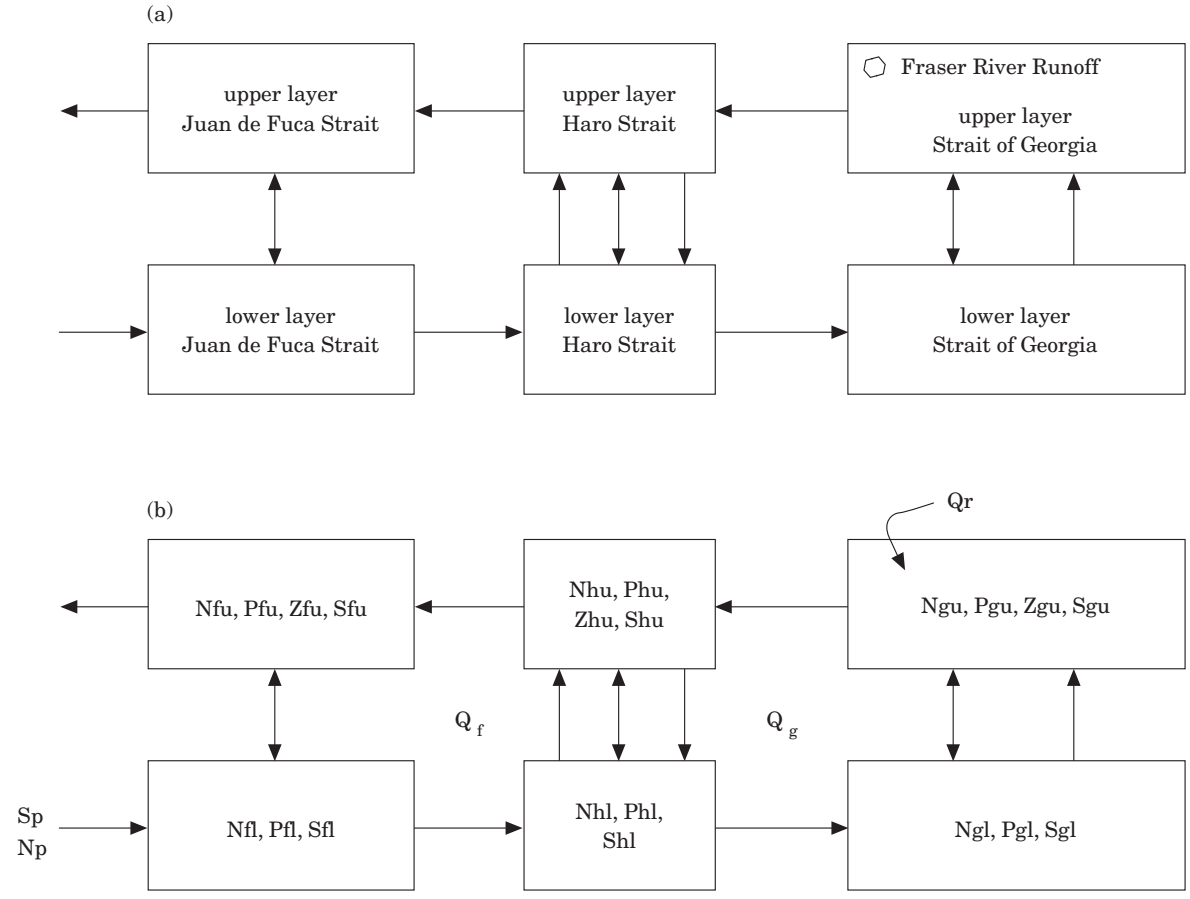

FIGURE 2. (a) Schematic of a box model for the Georgia–Fuca Estuary. The estuary is divided into Georgia, Haro and Fuca basins, each of which consists of an upper and a lower box. (b) Definition of symbols. Q_r represents the Fraser River runoff, S_p and N_p the Pacific salinity and nutrient concentration. Q_g is the volume flux between the Strait of Georgia and Haro Strait and Q_f the volume flux between Haro Strait and Juan de Fuca Strait.

$$V_{gu}\frac{dN_{gu}}{dt} = Q_g(N_{gl}-N_{gu}) + \omega_g A_g(N_{gl}-N_{gu}) - rP_{gu}\min\left(\frac{N_{gu}}{K_s+N_{gu}}, \frac{I}{i_b+I}\right)V_{gu}, \quad (6)$$

$$V_{gl}\frac{dP_{gl}}{dt} = Q_g(P_{hl}-P_{gl}) - \omega_g A_g(P_{gl}-P_{gu}) - p_{ml}P_{gl}V_{gl}, \quad (7)$$

$$V_{gl}\frac{dN_{gl}}{dt} = Q_g(N_{hl}-N_{gl}) - \omega_g A_g(N_{gl}-N_{gu}), \quad (8)$$

$$V_{hu}\frac{dP_{hu}}{dt} = Q_g(P_{gu}-P_{hu}) + Q_f(P_{hl}-P_{hu}) + \omega_h A_h(P_{hl}-P_{hu}) + rP_{hu}\min\left(\frac{N_{hu}}{K_s+N_{hu}}, \frac{I}{i_b+I}\right)V_{hu} - r_m\frac{{P_{hu}}^2 Z_{hu}}{K_p^2+{P_{hu}}^2}V_{hu} - p_m P_{hu}V_{hu}, \quad (9)$$

$$V_{hu}\frac{dZ_{hu}}{dt} = Q_g Z_{gu} - Q_f Z_{hu} + g_a r_m\frac{{P_{hu}}^2 Z_{hu}}{K_p^2+{P_{hu}}^2}V_{hu} - z_m Z_{hu}V_{hu}, \quad (10)$$

$$V_{hu}\frac{dN_{hu}}{dt} = Q_g(N_{gu}-N_{hu}) + Q_f(N_{hl}-N_{hu}) + \omega_h A_h(N_{hl}-N_{hu}) + rP_{hu}\min\left(\frac{N_{hu}}{K_s+N_{hu}}, \frac{I}{i_b+I}\right)V_{hu}, \quad (11)$$

$$V_{hl}\frac{dP_{hl}}{dt} = Q_g(P_{hu}-P_{hl}) + Q_f(P_{fl}-P_{hl}) - \omega_h A_h(P_{hl}-P_{hu}) - p_{ml}P_{hl}V_{hl}, \quad (12)$$

$$V_{hl}\frac{dN_{hl}}{dt} = Q_g(N_{hu}-N_{hl}) + Q_f(N_{fl}-N_{hl}) - \omega_h A_h(N_{hl}-N_{hu}), \quad (13)$$

$$V_{fu}\frac{dP_{fu}}{dt}=Q_f(P_{hu}-P_{fu})+\omega_f A_f(P_{fl}-P_{fu})+rP_{fu}\min\left(\frac{N_{fu}}{K_s+N_{fu}},\frac{I}{i_b+I}\right)V_{fu}-r_m\frac{{P_{fu}}^2 Z_{fu}}{K_p^2+{P_{fu}}^2}V_{fu}-p_m P_{fu}V_{fu}, \quad (14)$$

$$V_{fu}\frac{dZ_{fu}}{dt}=Q_f(Z_{hu}-Z_{fu})+g_a r_m\frac{{P_{fu}}^2 Z_{fu}}{K_p^2+{P_{fu}}^2}V_{fu}-z_m Z_{fu}V_{fu}, \quad (15)$$

$$V_{fu}\frac{N_{fu}}{dt}=Q_f(N_{hu}-N_{fu})+\omega_f A_f(N_{fl}-N_{fu})-rP_{fu}\min\left(\frac{N_{fu}}{K_s+N_{fu}},\frac{I}{i_b+I}\right)V_{fu}, \quad (16)$$

$$V_{fl}\frac{dP_{fl}}{dt}=Q_f(P_p-P_{fl})-\omega_f A_f(P_{fl}-P_{fu})-p_{ml}P_{fl}V_{fl}, \quad (17)$$

$$V_{fl}\frac{dN_{fl}}{dt}=Q_f(N_p-N_{fl})+\frac{1}{t_r}V_{fl}(N_p-N_{fl})-\omega_f A_f(N_{fl}-N_{fu}). \quad (18)$$

Because the phytoplankton population in the deep Pacific Ocean, P_p, is not known but expected to be small, we assume $P_p=P_{fl}$, the concentration in the deep box of Juan de Fuca Strait.

Annual variation of salinity and nutrient concentrations in the continental shelf waters off Vancouver Island results from upwelling and downwelling cycles caused by seasonal changes in wind direction along the coast (Thomson, 1981). The seasonal cycle of the shelf salinity is thus prescribed to be

$$S_p=S_{p0}+\Delta S_p sech^2\left[10\frac{(t-T/2-t_l)}{T}\right] \quad (19)$$

in which T is the length of a year, S_{p0} is the low winter salinity and ΔS_p is the amplitude of the seasonal variation. Upwelling is usually most vigorous in August, lagging the freshet by $t_l\approx 2$ months. Mackas and Harrison (1997) showed that nitrate correlates with salinity at depths below 50 m. Hence we specify the offshore Pacific nitrate concentrations as a linear function of salinity,

$$N_p=3{\cdot}4S_p-78{\cdot}3 \quad (20)$$

such that N_p varies between 32·2 and 39 mmol Nm^{-3} when S_p varies between 32·5 and 34·5. The nutrient and salinity in the deep box of the Juan de Fuca Strait are relaxed to N_p and S_p, respectively, with a relaxation time scale of about $t_r=2$ months.

The model considers the daily-averaged phytoplankton growth rate with a typical doubling time of a couple of days. We include the effect of light limitation on phytoplankton growth [cf. Equation (1)]. In clear sky at latitude 50°, the daily-averaged short-wave radiation at the ocean surface varies from 50 Wm^{-2} in winter to 300 Wm^{-2} in summer (e.g. Figure 5.5 in Pickard & Emery, 1990). Clouds, particularly during rainy winter months, reduce the direct solar radiation but increase the proportion of sky radiation in the photosynthetic range. For a cloud cover of 6 oktas, there is about 25% reduction in the incoming radiation. Once light penetrates into the water column, it attenuates rapidly in coastal waters. The seasonal variation of the depth-averaged PAR in the upper box is given by

$$I(t)=I_w+\frac{I_s-I_w}{2}\left[1-\cos\frac{2\pi t}{T}\right] \quad (21)$$

where we take $I_w=5$ Wm^{-2} to be the winter PAR value and $I_s=200$ Wm^{-2} the summer PAR value. We choose i_b so that in the winter phytoplankton grow at about 10% of the maximum rate and the summer light level is saturated. The model assumes that the depth of upper boxes is fixed. However, the euphotic layer in the Strait of Georgia becomes shallower during summer freshet so that phytoplankton are exposed to higher light levels and smaller nutrient pool. To account for this effect, we scale the ‘ effective euphotic layer thickness ’ in the Strait of Georgia by the salinity difference (stratification) between the upper and lower boxes, relative to the winter (minimum) difference, i.e. we replace I with $I^e=I\Delta S_g/\Delta S_{gw}$ and N_{gu} with $N^e_{gu}=N_{gu}\Delta S_{gw}/\Delta S_g$ in the phytoplankton growth functions in Equations 4 and 6. Here $\Delta S_g=S_{gl}-S_{gu}$ is the vertical stratification in the Strait of Georgia and ΔS_{gw} is its winter minimum value.

Nondimensionalizing equations reduces the number of parameters in the model. There are five dimensionless biological parameters: (1) $b_1=rt_s$ is the ratio of time scale of estuarine circulation to phytoplankton doubling time; (2) $b_2=g_a r_m/r$ is the ratio of maximum zooplankton growth rate to maximum phytoplankton growth rate; (3) $b_3=p_m/r$ is the ratio of phytoplankton mortality rate to its maximum growth rate; (4) $b_4=z_m/(g_a r_m)$ is the ratio of zooplankton mortality rate to maximum zooplankton growth rate; (5) $b_5=K_s/K_p$ compares the half-saturation constant for nutrient uptake to that for zooplankton grazing. The parameter $b_{3l}=p_{ml}/r$ is the ratio of phytoplankton

TABLE 1. Dimensional and nondimensional biological parameters used in the model runs

Parameter	Symbol	Units	Run 1	Run 2	Run 3	Range
Phytoplankton maximum growth rate	r	day^{-1}	0·435	0·435	0·435	0·217 to 1·3
Phytoplankton mortality rate	p_m	day^{-1}	0·0435	0·0435	0·087	0·0217 to 0·109
Phytoplankton mortality rate in aphotic deep water	p_{ml}	day^{-1}	0·174	0·174	0·174	0·0868 to 0·52
Nutrient half-saturation constant	K_s	mmol Nm^{-3}	1·5	1·5	1·5	1 to 2
Zooplankton maximum grazing rate	r_m	day^{-1}	0·174	0·087	0·174	0·0289 to 0·867
Zooplankton grazing efficiency	g_a		0·75	0·75	0·75	
Zooplankton grazing half-saturation constant	K_p	mmol Nm^{-3}	1·5	1·5	1·5	1 to 2
Zooplankton mortality rate	z_m	day^{-1}	0·0131	0·0065	0·0261	0·0065 to 0·0326
rt_s	b_1		1	1	1	0·5 to 3
$g_a r_{m/r}$	b_2		0·3	0·15	0·3	0·1 to 0·5
$p_{m/r}$	b_3		0·1	0·1	0·2	0·05 to 0·25
$p_{ml/r}$	b_{31}		0·4	0·4	0·4	0·4
$z_m/(g_a r_m)$	b_4		0·1	0·1	0·2	0·05 to 0·25
K_s/K_p	b_5		1	1	1	1

death rate in aphotic deep water to its growth rate in the euphotic layer. We choose $b_{3l}=0·4$ such that the deep phytoplankton population decreases by a factor of 100 in a month. Although we explore model runs in the more compact nondimensional parameter space, we shall present model results in dimensional units.

Annual cycle of plankton population and nutrient concentration

The coupled biological–physical model is run for a standard set of physical (see Appendix) and biological parameters: $b_1=1$, $b_2=0·3$, $b_3=0·1$, $b_4=0·1$, $b_5=1$ (see Run 1 in Table 1). These correspond to a phytoplankton growth rate of 0·43 day^{-1}, a zooplankton growth rate of 0·13 day^{-1}, a phytoplankton mortality rate of 0·043 day^{-1}, a zooplankton mortality rate of 0·013 day^{-1} and $K_s=K_p=1·5$ mmol Nm^{-3}.

Figure 3(a, c) shows the seasonal cycle of salinities and volume fluxes (see also Appendix). Although nutrient is transported (and mixed) in the same way as salt, the seasonal cycle of nutrient concentration is different from that of salinity, as shown in Figure 3(b). In spring there is a large drawdown of nutrient in the euphotic layer of the Strait of Georgia but smaller drawdowns in the other two straits. It is interesting to note that the nutrient concentration in the euphotic layer of Juan de Fuca Strait stays well above the limiting level, in apparent agreement with observations (Mackas & Harrison, 1997). Strong upwelling in late summer over the continental shelf recharges the estuary with high salinity, high nutrient water via the deep estuarine inflow. It takes longer to restore the nutrient concentration in the upper box of the Strait of Georgia than in Haro and Juan de Fuca Straits.

The seasonal development of plankton populations will now be examined in each of the three basins. As Figure 4(a) shows, a large spring bloom develops in the Strait of Georgia in March, followed by a rising zooplankton population. In contrast, the phytoplankton population remains small in the Haro Strait [Figure 4(b)]. Despite high nutrient levels in the euphotic layer of Juan de Fuca Strait, the phytoplankton population remains relatively small throughout the year [Figure 4(c)]. However, zooplankton populations are of the same order of magnitude across the three basins.

One critical question regarding the phytoplankton production is whether it is light-limited or nutrient-limited. Generally speaking, phytoplankton production would be expected to be macro-nutrient-limited in a Southern regime such as the California and Oregon coasts and light-limited in a Northern regime such as the Alaskan coast (Gargett, 1997). Geographically the Vancouver Island coast is located in the transition between the two regimes. We present the instantaneous functions for light utilization $[I/(i_b+I)]$ and nutrient uptake $[N/(K_s+N)]$ in Figure 5. With the standard choice of i_b and K_s, phytoplankton growth is light-limited in all three basins during the winter season. However, in the Strait of Georgia, phytoplankton production switches to nutrient limitation during the summer. In contrast, light is always the limiting factor in Haro Strait and Juan de Fuca Strait. In this sense, Juan de Fuca Strait and Haro Strait belong to the Northern regime and the Strait of Georgia to the Southern regime.

Population size is a quantity describing plankton standing stocks, but an equally important quantity is the production rate or productivity. The gross primary

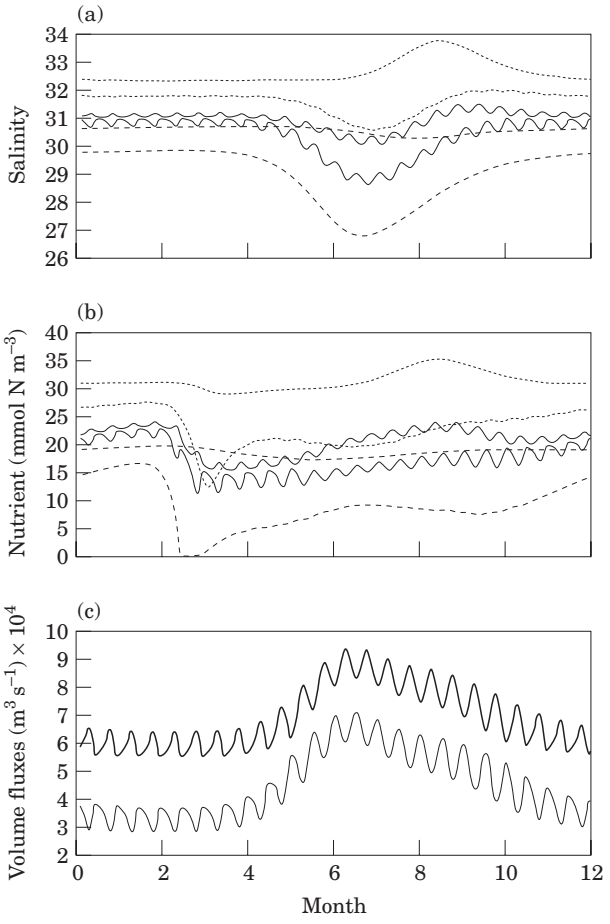

FIGURE 3. (a) Seasonal variations of (a) salinities, (b) nutrient concentration (dashed lines correspond to the Strait of Georgia, solid lines to Haro Strait and dotted lines to the Juan de Fuca Strait. Larger values of salinity and nutrient concentration represent lower boxes.), (c) volume fluxes Q_g between Georgia and Haro basins (thin solid) and Q_f between Haro and Fuca basins (thick solid) where Q_f has been offset by 3 units for visual clarity. Biological parameters are set at $b_1=1$, $b_2=0{\cdot}3$, $b_3=0{\cdot}1$, $b_4=0{\cdot}1$ and $b_5=1$ (see Run 1 in Table 1).

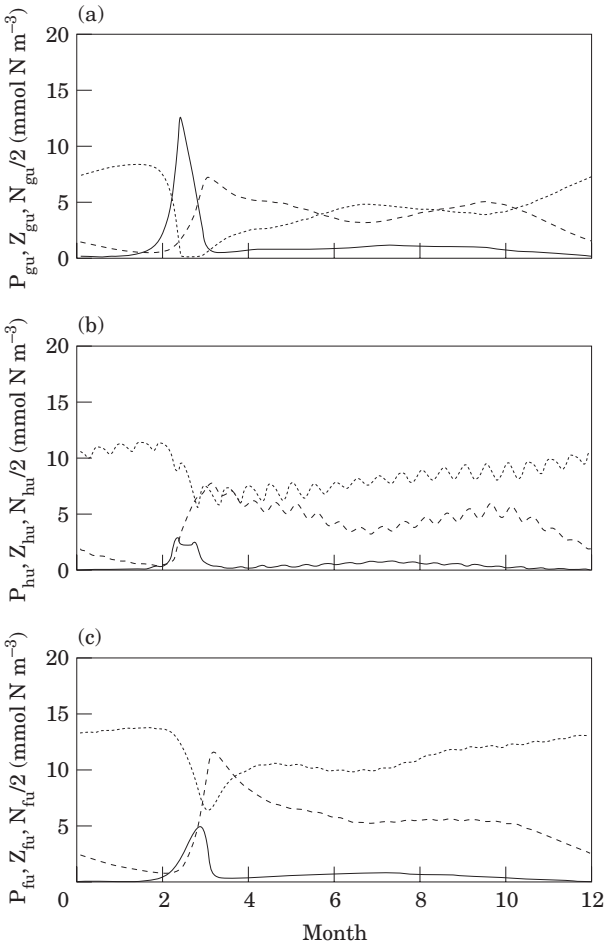

FIGURE 4. Seasonal variation of phytoplankton (solid), zooplankton (dashed) populations and nutrient concentration (dotted) in (a) the Strait of Georgia, (b) Haro Strait and (c) Juan de Fuca Strait [corresponds to Run 1 in Figure 14(e)].

productivity (for phytoplankton) and secondary productivity (for zooplankton) is calculated for each of the three basins. In order to compare with measurements, the rates over depth are integrated and converted from nitrogen to carbon units using the standard Redfield ratio. The primary productivity peaks between March and April while the secondary productivity peaks slightly later. We calculate the total annual primary production per unit area. The Strait of Georgia has the highest annual production of about 377 g Cm^{-2} year^{-1}, followed by Juan de Fuca Strait at 303 g Cm^{-2} year^{-1} and Haro Strait at 238 g Cm^{-2} year^{-1}. The secondary production is only a fraction of the primary production because a fraction of phytoplankton is lost to natural mortality and unassimilated grazing and hence is not transferred to the higher trophic level.

These model predictions are in reasonable agreement with observations. Harrison *et al.* (1983) summarized biological data collected in the Strait of Georgia. Monthly averages of nitrate concentration in the top 20 m range from 22 mmol Nm^{-3} in the winter to about 8 mmol Nm^{-3} in the summer. At some measurement stations, nitrate temporarily dropped to under 1 mmol Nm^{-3}. Chlorophyll *a* concentration ranges from <1 mg m^{-3} in the winter to >15 mg m^{-3} during the spring. With a unit conversion from 1 mg m^{-3} chlorophyll *a* to 1 mmol Nm^{-3}, phytoplankton concentration varies between 1 and 15 mmol Nm^{-3} in the Strait of Georgia. Zooplankton biomass reached a maximum of 1·4 g wet wt m^{-3} in May and dropped down to <0·05 g wet wt m^{-3} in

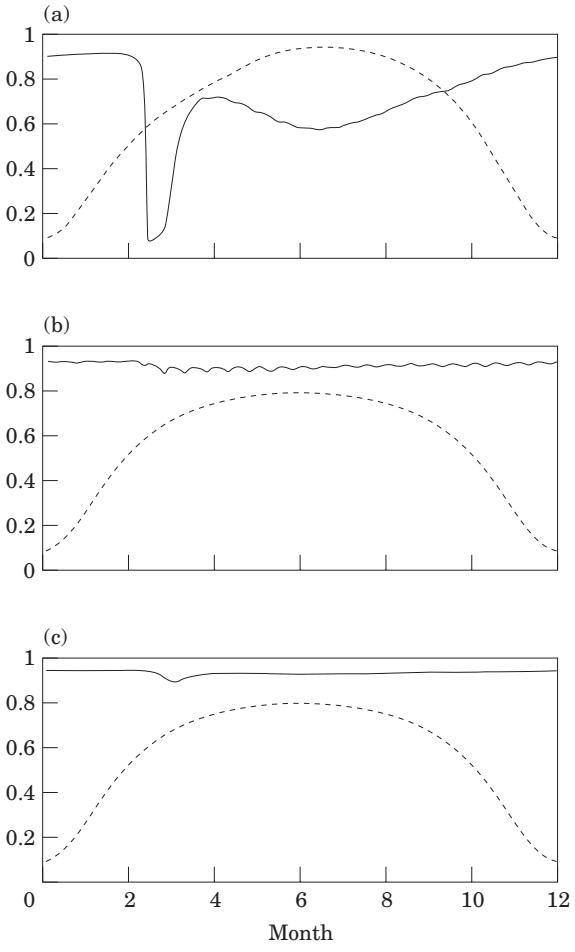

FIGURE 5. Comparison between nutrient uptake function (solid) and light utilization function (dashed) for (a) the Strait of Georgia, (b) Haro Strait and (c) Juan de Fuca Strait.

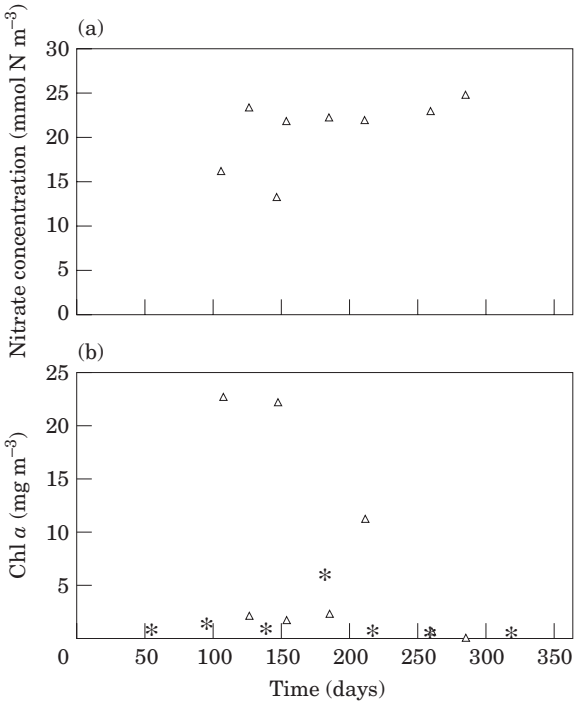

FIGURE 6. Observations of nitrate (a) and chlorophyll *a* (b) concentrations in Juan de Fuca Strait. Symbol (△) denotes data collected at IOS (e.g. Hill *et al.*, 1982) and symbol (*) denotes data collected by NOAA (Chester *et al.*, 1977).

the winter in the surface water. With a unit conversion from 1 g wet wt m^{-3} to 5 mmol Nm^{-3}, zooplankton concentration varies between <0·25 and 7 mmol Nm^{-3}. Primary production varies considerably over different stations in the Strait of Georgia. Stockner *et al.* (1979) gave an estimate of 280 g Cm^{-2} year^{-1} for the annual primary productivity averaged over the strait. (They chose a conservative estimate rather than the average from all stations which gives 345 g Cm^{-2} year^{-1}.) Stockner *et al.* (1979) compared chlorophyll *a* concentration and algal volume between a station in the Strait of Georgia and one in Haro Strait and found that phytoplankton population in Haro Strait was between one-tenth and one-quarter of its counterpart in the Strait of Georgia.

There are few published reports on plankton and nutrient measurements in Juan de Fuca Strait. Chester *et al.* (1977) obtained chlorophyll *a* measurements over nine stations in Juan de Fuca Strait at monthly intervals during 1976, but they did not obtain nutrient measurements. The Institutes of Ocean Sciences collected chemical and biological data in Juan de Fuca Strait over many years (e.g. Hill *et al.*, 1982), but data collected over any one year were not sufficient to resolve an annual cycle and sampling stations also varied between years. To compare with model results, we calculate algebraic means of all nitrate and chlorophyll *a* data in the surface waters (down to 50 m depth) of Juan de Fuca strait. The data are compiled from observations in different years and the scatter of data points may be partly related to interannual variability. As shown in Figure 6(a), nitrate concentration averages to about 22 mmol Nm^{-3} in the surface layer of Juan de Fuca Strait and does not fall down to the limiting level (1 to 2 mmol Nm^{-3}). The chlorophyll *a* concentration is usually low (under 2 mg m^{-3}), although it exceeds 20 mg m^{-3} in a couple of observations during the spring bloom (see below for a discussion). When comparing the three figures in Figure 4, one notices that zooplankton populations are of similar size in the three straits despite large differences in phytoplankton population. These results agrees with the biological

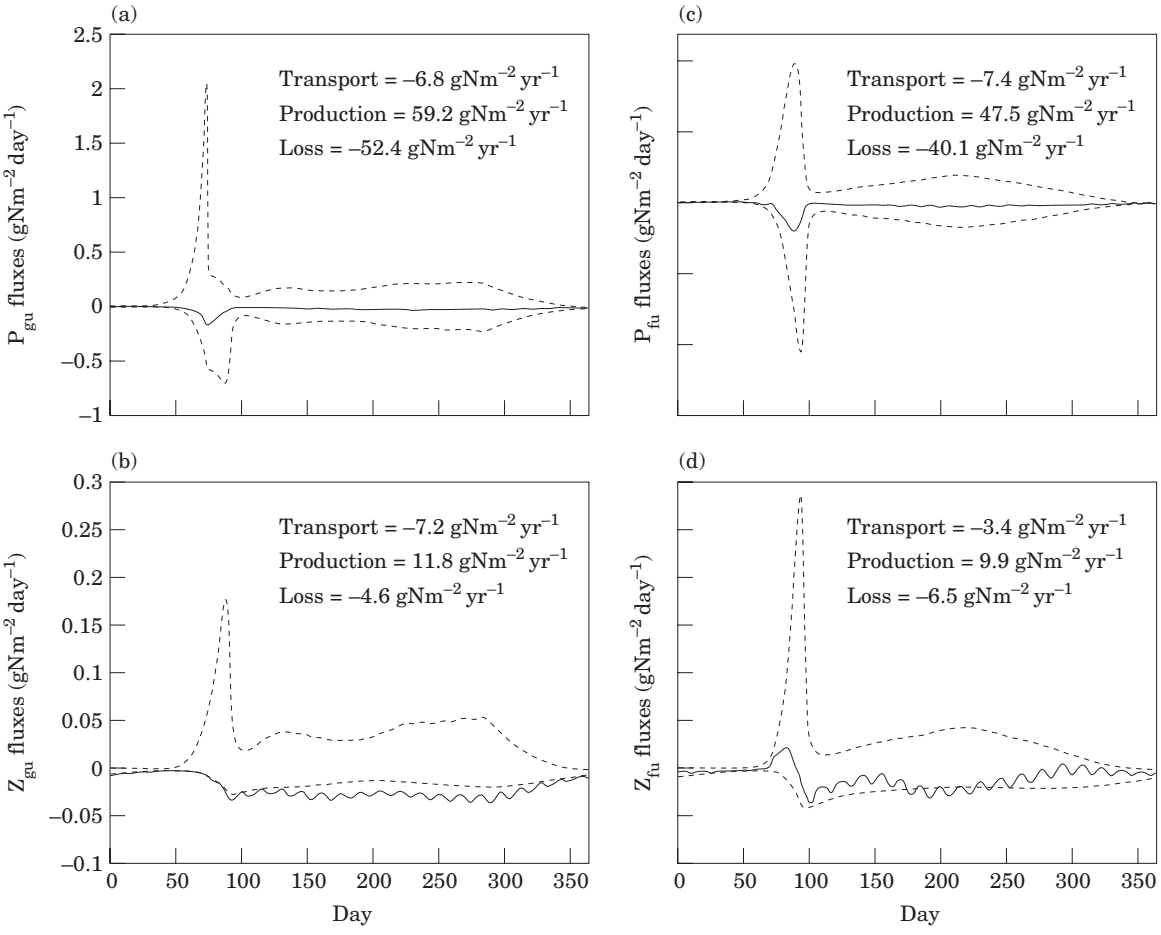

FIGURE 7. Comparison between physical transport term (solid), biological production (dashed and positive) and biological losses (dashed and negative) for phytoplankton and zooplankton in the Strait of Georgia (a and b) and in the Juan de Fuca Strait (c and d).

sampling of phytoplankton and zooplankton in an along-strait cross-section (Denman *et al.*, 1981).

Effect of estuarine circulation on plankton production

The estuarine circulation transports nutrients and plankton between the basins. How does this transport affect the plankton production? In Equations 4 to 18, we can classify terms on the right hand side of each equation into three types: (1) physical transport including vertical mixing and advection; (2) biological production; and (3) biological losses. We now compare these terms for phytoplankton and zooplankton in each of the three upper boxes in the model.

Figure 7(a, b) shows a comparison of these terms in the euphotic layer of the Strait of Georgia. For phytoplankton, as shown in Figure 7(a), there is a pronounced peak in production during the spring bloom in March. This is followed by a peak in biological losses due to grazing by zooplankton. In comparison, the physical transport term is quite small. When integrated over a year, biological production amounts to $59{\cdot}2\ \mathrm{g\,Nm^{-2}\ year^{-1}}$ whereas biological losses account for $-52{\cdot}4\ \mathrm{g\,Nm^{-2}\ year^{-1}}$. Hence, phytoplankton production in the Strait of Georgia is primarily a local process where production is balanced by losses. The transport by the estuarine circulation plays a minor role. However, both biological losses and physical transport are important in balancing the production of zooplankton [Figure 7(b)]. The removal of zooplankton due to estuarine outflow is in fact the dominant loss term, implying that a large mass of zooplankton is advected out of the Strait of Georgia. This will have an important impact on the foodweb system in Haro and Juan de Fuca Straits. The phytoplankton doubling time of a couple of days is usually much shorter than the time scale of the estuarine circulation (e.g. the flushing time for the upper layer of the Strait of Georgia is estimated to be

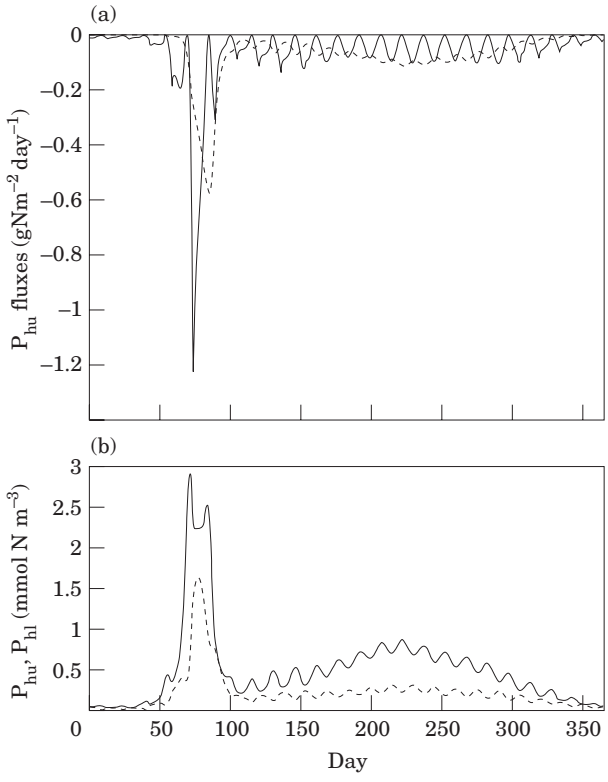

FIGURE 8. Phytoplankton in Haro Strait. (a) Comparison between vertical mixing (solid) and zooplankton grazing terms (dashed). (b) Time series of phytoplankton populations in the euphotic upper layer (solid) and in the aphotic lower layer (dashed).

46 days at a peak volume flux of 5×10^4 m^3 s^{-1}). Hence, the slow advection by the estuarine circulation is less important. However, zooplankton grow at a slower rate with a doubling time of about 10 days or longer. During this period, the estuarine outflow removes a significant fraction of zooplankton from the Strait of Georgia.

As shown in Figure 4(b), the phytoplankton population in Haro Strait remains small throughout the year. To ascertain what is responsible for maintaining such a small stock, the removal of phytoplankton due to vertical mixing [$\omega_h A_h(P_{hl} - P_{hu})$ in Equation 9] is compared with that due to grazing [$-r_m P_{hu}^2 Z_{hu} V_{hu}/(K_p^2 + P_{hu}^2)$ in Equation 9] in Figure 8(a). The periodic loss of phytoplankton to the aphotic lower layer by tidal mixing appears to be an important loss term. As shown in Figure 8(b), phytoplankton population in the lower box of the Haro Strait is of comparable magnitude to that in the upper box, confirming continuing losses to the lower box by tidal mixing.

Despite high nutrient concentrations, no significant spring blooms develops in the upper layer of Juan de Fuca Strait. Unlike in the Strait of Georgia [see Figure 7(a)], there is virtually no time delay between the peak phytoplankton production and peak zooplankton grazing [see Figure 7(c)] so that zooplankton grazing has kept in phase with the phytoplankton production. Apparently, the advection of zooplankton from the inner straits to Juan de Fuca Strait provides a sufficient seed population in the spring allowing the zooplankton population to respond rapidly as phytoplankton production increases [see Figure 7(d)]. Other hypotheses have been proposed to explain the high nutrient low chlorophyll regime in the Fuca euphotic layer. It was suggested (D. L. Mackas (1998), pers. comm.) that the surface layer depth in the Fuca basin (in the range of 50 to 100 m) may be deeper than the critical depth for phytoplankton production so that there is no net phytoplankton growth. Further observations are needed to test these alternative hypotheses.

The nutrient budget is examined for the whole Georgia–Fuca Estuary. Figure 9 shows the time series of nutrient influx from the Pacific Ocean, nutrient outflux from the upper layer of Juan de Fuca Strait and biological uptake in the Georgia, Fuca and Haro Basins. Both the advective influx and outflux reach maximum values in the summer when the estuarine circulation is strongest. The biological uptake occurs mainly in the spring time. The averaged influx is 1868 tonnes N day^{-1}. Half the imported nutrients are advected out, with the averaged outflux at about -987 tonnes N day^{-1}. The Strait of Georgia takes up about -691 tonnes N day^{-1}, Haro Strait -52 tonnes N day^{-1} and Juan de Fuca Strait -288 tonnes N day^{-1}. These model calculations are in reasonable agreement with the annual budget estimates of Mackas and Harrison (1997). In addition, our model indicates marked seasonal cycles of these fluxes to be expected.

Ecosystem response to interannual variability in estuarine circulation

Historical records show that the Fraser River runoff exhibits considerable interannual variability (Thomson, 1994). This variability appears to be related to large-scale climate variability in the North Pacific, which also affects shelf water properties (Ebbesmeyer *et al.*, 1989; Cayan & Peterson, 1989). Li *et al.* (1999) showed that the estuarine circulation in the Georgia–Fuca Estuary responds rapidly (within a year) to interannual variability in both river runoff and shelf water salinity. Now we examine how the modelled planktonic ecosystem in the Georgia–Fuca Estuary responds to this variability.

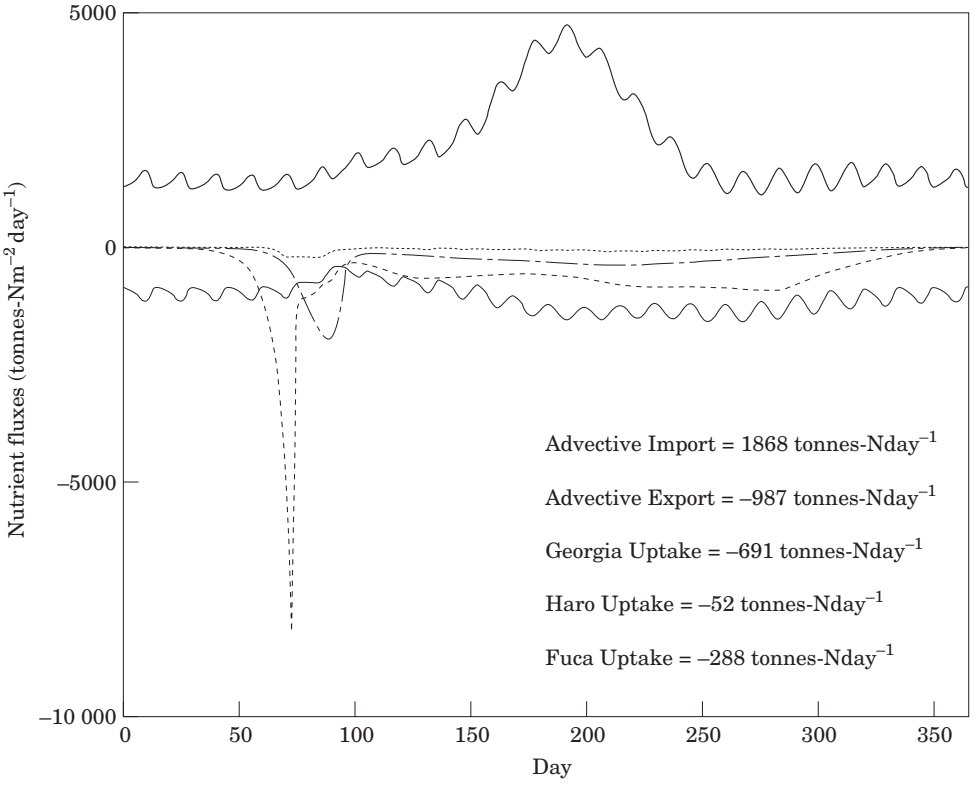

FIGURE 9. Total nutrient budget for the Georgia–Fuca Estuary. The positive solid line represents deep nutrient input from the Pacific Ocean while the negative solid line nutrient export from the upper layer of Juan de Fuca Strait. The dashed line represents nutrient uptake in the Strait of Georgia, dotted line nutrient uptake in Haro Strait and dash-dot line nutrient uptake in Juan de Fuca Strait.

As a first step, a number of simulations are carried out for different combinations of Fraser River runoff and shelf water salinity, i.e. different values of Q_{rs} and ΔS_p. Larger values of Q_{rs} correspond to higher runoffs during the summer freshet and larger values of ΔS_p correspond to larger seasonal fluctuations of the shelf salinity. It was found that the peak phytoplankton populations during spring blooms change by about 40% as Q_{rs} varies by a factor of 4 or ΔS_p by a factor of 3. The changes in the zooplankton populations are smaller. These results indicate a moderate variation of plankton stocks for the observed ranges of river runoff and salinity variability.

To simulate realistic interannual variability in the estuarine circulation, a stochastic function is used to represent Fraser River runoff, Q_r, in which peak runoff, start-time and duration of the freshet vary randomly within observed ranges. We also use a stochastic function to represent the shelf salinity S_p (see Li *et al.*, 1999). Figure 10 shows a sample simulation over a five year period. Not surprisingly, N_{fl} (in the lower Juan de Fuca box) closely tracks the nutrient concentration on the shelf, N_p (which is linearly proportional to S_p). The nutrient distribution in Haro Strait also changes as a direct result of the variability in the estuarine circulation. However, the phytoplankton and zooplankton populations change only marginally from year to year. Hence the modelled planktonic ecosystem appears to be relatively insensitive to observed levels of interannual variability in the physical system.

Model sensitivity to biological parameters

Observations have shown that plankton populations (and production) in the estuary vary from year to year. For example, Stockner *et al.* (1979) took monthly samples of phytoplankton and zooplankton in the Strait of Georgia: they found a small spring bloom and large zooplankton stocks in 1975 but large phytoplankton biomass and low zooplankton stocks in 1976. If changes in estuarine circulation only have a small impact on the planktonic ecosystem, what determines the interannual variability of plankton production? This section covers the sensitivity of the planktonic ecosystem to variations in biological parameters. For a coastal planktonic ecosystem such as that in the Georgia–Fuca basin, the half-saturation

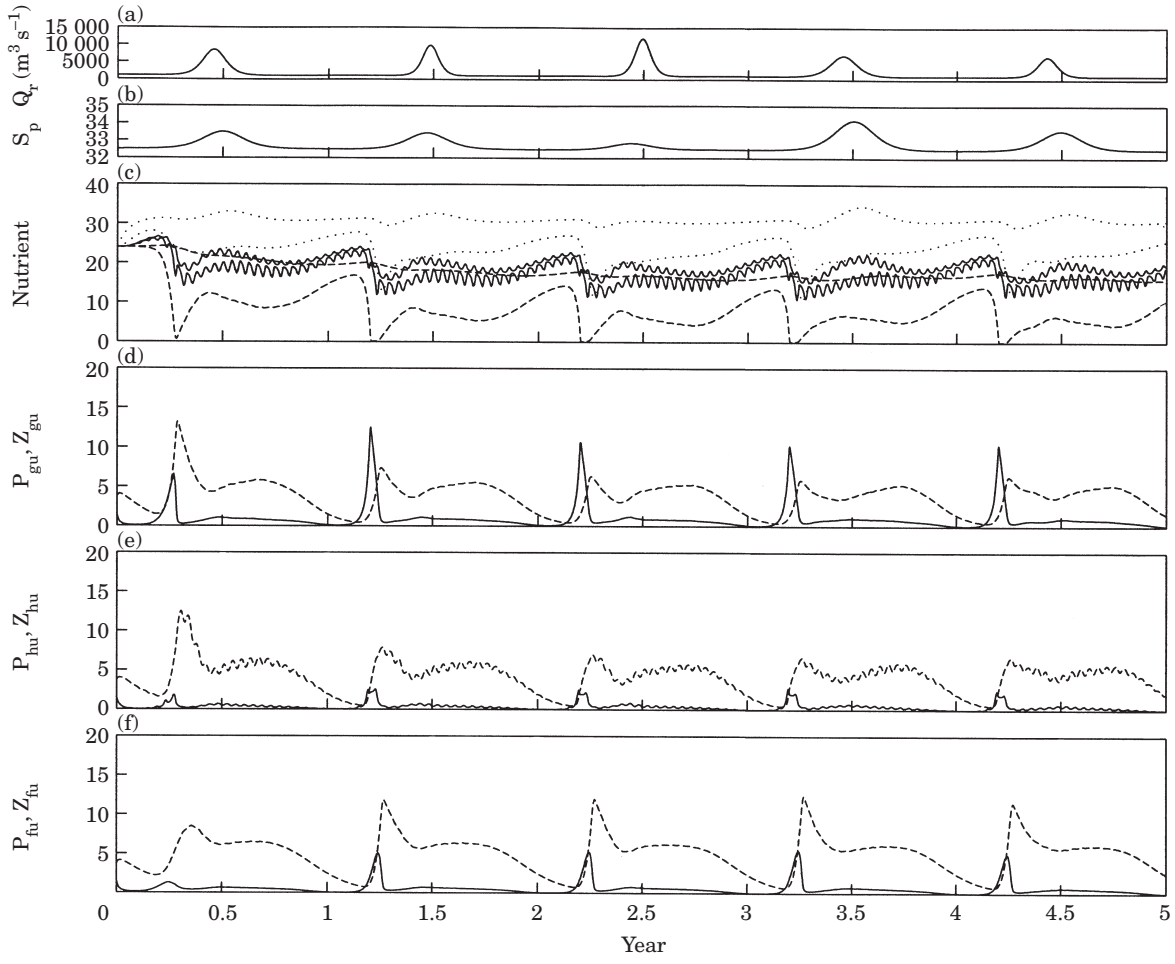

FIGURE 10. Ecosystem response to interannual variability of estuarine circulation simulated by stochastically varying Fraser River runoff and shelf salinity fluctuations. (a) Fraser River runoff, (b) shelf salinity, and (c) nutrient concentration in the Strait of Georgia (dashed), Haro Strait (solid) and Juan de Fuca Strait (dotted). Phytoplankton (solid) and zooplankton (dashed) populations in (d) the Strait of Georgia, (e) Haro Strait and (f) Juan de Fuca Strait. All biological variations are in units of mmol Nm^{-3}.

coefficient for nutrient uptake K_s varies over 1 to 2 mmol Nm^{-3} (Mackas & Harrison, 1997) and the corresponding coefficient for zooplankton grazing K_p from 1 to 2 mmol Nm^{-3} (Mackas, 1998, pers. comm.) so that $b_5 = K_s/K_p \approx 1$. Hence in the following model runs we shall fix $b_5 = 1$ and $K_s = K_p = 1{\cdot}5$ mmol Nm^{-3}. To explore the parameter space consisting of the remaining four dimensionless biological parameters (b_1 to b_4), we examine variations of two parameters at a time.

First we examine the model sensitivity to the growth rate parameters of phytoplankton and zooplankton, b_1 and b_2, while holding their respective relative mortality rates at standard values of $b_3 = b_4 = 0{\cdot}1$. Figure 11 shows the contours of annual mean primary $PP = rPmin(N/(K_s+N),\ I/(i_b+I))$ and secondary $SP = g_a r_m P^2 Z/(K_p^2+P^2)$ productivity rates for the Strait of Georgia and Juan de Fuca Strait. Not surprisingly, the primary productivity in both straits decreases when either phytoplankton growth rate decreases or zooplankton growth rate increases, whereas the secondary productivity increases as either b_1 or b_2 increases. It is interesting to note that the primary productivity in the Strait of Georgia is nearly constant in the upper left quadrant of the parameter space. Examination of the nutrient concentration shows that there is a more extensive period of nutrient limitation in the Strait of Georgia at a larger value of b_1 so that the primary productivity remains approximately constant.

The estuarine circulation transports plankton between the Strait of Georgia and Juan de Fuca Strait, thus leading to rather different parameter dependencies of plankton standing stocks in the two straits, as

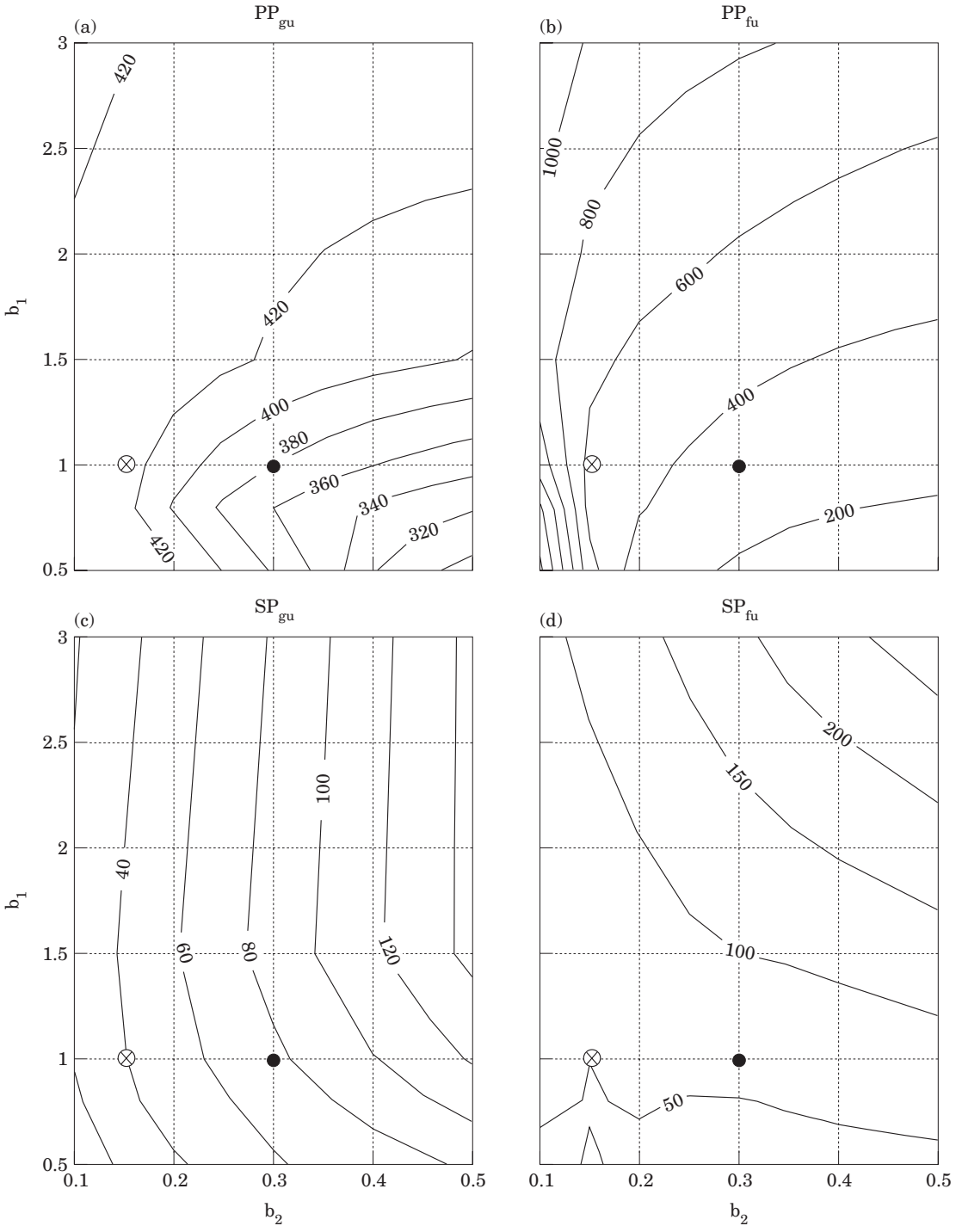

FIGURE 11. Sensitivity of the ecosystem to plankton growth parameters b_1 and b_2. Contours of primary productivity in (a) the Strait of Georgia and in (b) Juan de Fuca Strait. Contours of secondary productivity in (c) the Strait of Georgia and in (d) Juan de Fuca Strait. All variables are in units of g Cm^{-2} $year^{-1}$. Symbol (●) corresponds to Run 1 and (⊗) to Run 2 in Figure 12(e).

shown in Figure 12. We choose the peak phytoplankton populations during the spring bloom, $Max(P_{gu})$ and $Max(P_{fu})$, and the annually-averaged zooplankton populations, $Mean(Z_{gu})$ and $Mean(Z_{fu})$, as key ecosystem indices. In the Strait of Georgia, the peak phytoplankton population size shows an inverse relationship

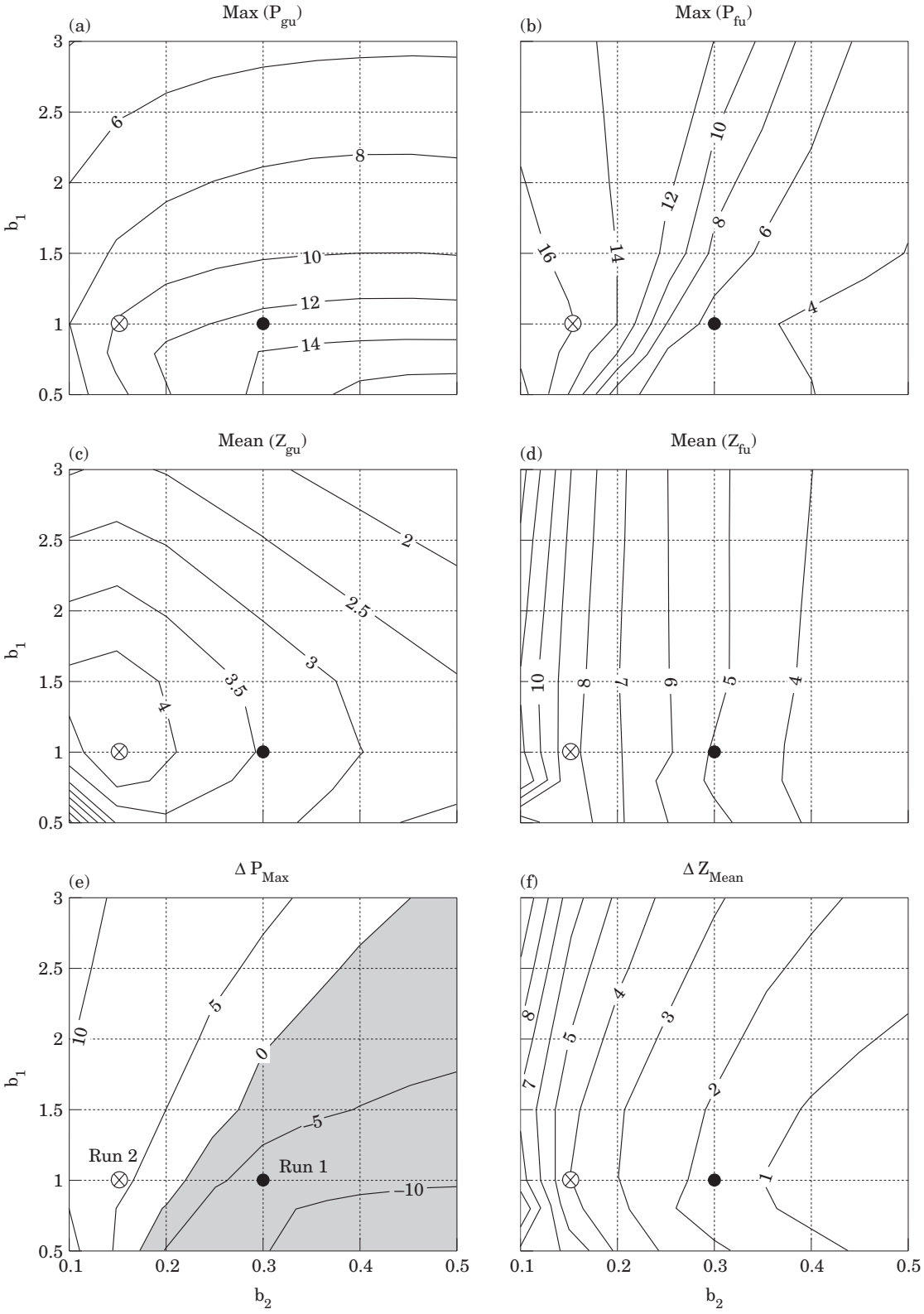

FIGURE 12. Sensitivity of the ecosystem to plankton growth parameters b_1 and b_2. Contours of peak phytoplankton populations in (a) the Strait of Georgia and in (b) Juan de Fuca Strait. Contours of annually-averaged zooplankton populations in (c) the Strait of Georgia and in (d) Juan de Fuca Strait. Contours of (e) ΔP_{max} and (f) ΔZ_{mean}. Point Run 1 (●) corresponds to the model run presented in Figure 4 and point Run 2 (⊗) to that in Figure 13. All variables are in units of mmol Nm^{-3}

with the primary productivity [cf. Figure 12(a) with Figure 11(a)]. Although the phytoplankton productivity during the spring bloom contributes significantly to the total annual primary production, the size of the spring bloom depends on factors such as the time delay (phase lag) between peak phytoplankton growth and peak zooplankton grazing. Figure 12(a) suggests that, in the Strait of Georgia, when phytoplankton grow at a faster rate, they support a greater late winter population of zooplankton such that increased zooplankton grazing results in a smaller spring phytoplankton bloom. However, the planktonic ecosystem in Juan de Fuca Strait is different. The estuarine outflow carries zooplankton from the Strait of Georgia to Juan de Fuca Strait, thus providing a seed population upon which zooplankton can grow. There is virtually no time delay between peak phytoplankton production and peak zooplankton grazing. Hence, the larger the grazing rate (b_2), the smaller the phytoplankton bloom size in this strait [Figure 12(b)]. Although one would think that the annually-averaged zooplankton population would increase with increasing grazing rate, Figure 12(c, d) shows that they actually decrease with b_2. This apparent contradiction results because the estuarine outflow in the euphotic layer causes a net loss of zooplankton in both the Strait of Georgia and Juan de Fuca Strait. Increasing zooplankton standing stocks implies larger advective losses, resulting in a net decrease of $Mean(Z_{gu})$ and $Mean(Z_{fu})$ with b_2.

Figure 12(e, f) shows the differences $\Delta P_{max} = Max(P_{fu}) - Max(P_{gu})$ and $\Delta Z_{mean} = Mean(Z_{fu}) - Mean(Z_{gu})$ between Juan de Fuca Strait and Strait of Georgia. There is a nearly-diagonal line at which the peak phytoplankton populations are the same in the two basins. To the right of this line, Regime 1, there is a larger phytoplankton bloom in the Strait of Georgia. To the left of this line, Regime 2, there is a larger phytoplankton bloom in Juan de Fuca Strait. With a typical phytoplankton doubling time of a couple of days (1 day corresponds to $\beta_1 \approx 1{\cdot}6$) and a ratio of zooplankton growth rate to phytoplankton growth rate between 30% and 40%, the phytoplankton stocks are mostly in Regime 1, as currently observed (Harrison *et al.*, 1983; Mackas & Harrison, 1997). Figure 12(f) shows that the zooplankton population in Juan de Fuca Strait is always greater than that in the Strait of Georgia.

Details of annual cycles of phytoplankton and zooplankton populations are presented in Figure 4 and Figure 13 (see Table 1). Figure 4 (Run 1) shows the time series of phytoplankton and zooplankton populations believed to be representative of the present-day plankton ecosystem in the Georgia–Fuca Estuary.

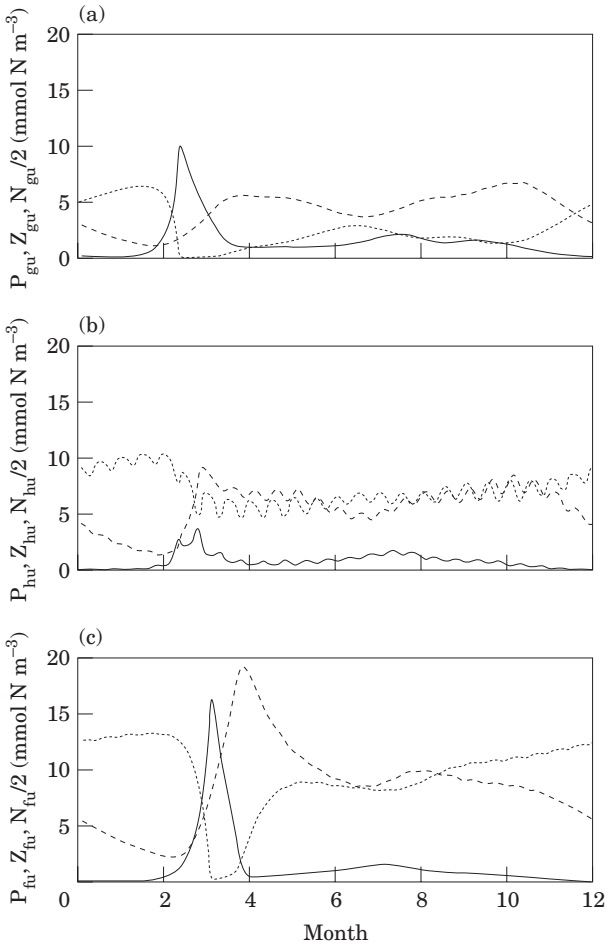

FIGURE 13. Seasonal variation of phytoplankton (solid), zooplankton (dashed) populations and nutrient concentration (dotted) in (a) the Strait of Georgia, (b) Haro Strait and (c) Juan de Fuca Strait [corresponds to Run 2 in Figure 12(e)].

There is a large spring bloom and nutrient limitation in the Strait of Georgia. Despite high nutrient levels in Juan de Fuca Strait, no significant spring bloom occurs there. Figure 13 (Run 2) shows the same time series typical of Regime 2. In this regime, there is a much larger phytoplankton bloom and associated larger zooplankton standing stock in Juan de Fuca Strait. Nutrient limitations extends for a longer period in the Strait of Georgia, thus limiting the size of the spring phytoplankton bloom.

In the next two figures, we examine how the planktonic ecosystem responds to changes in the phytoplankton and zooplankton mortality rates b_3 and b_4, while the growth rate parameters $b_1 = 0{\cdot}1$ and $b_2 = 0{\cdot}3$ are held fixed. Figure 14 shows that increasing zooplankton mortality rate releases phytoplankton from the grazing pressure and thus leads to higher annual primary productivity in both straits. On the other

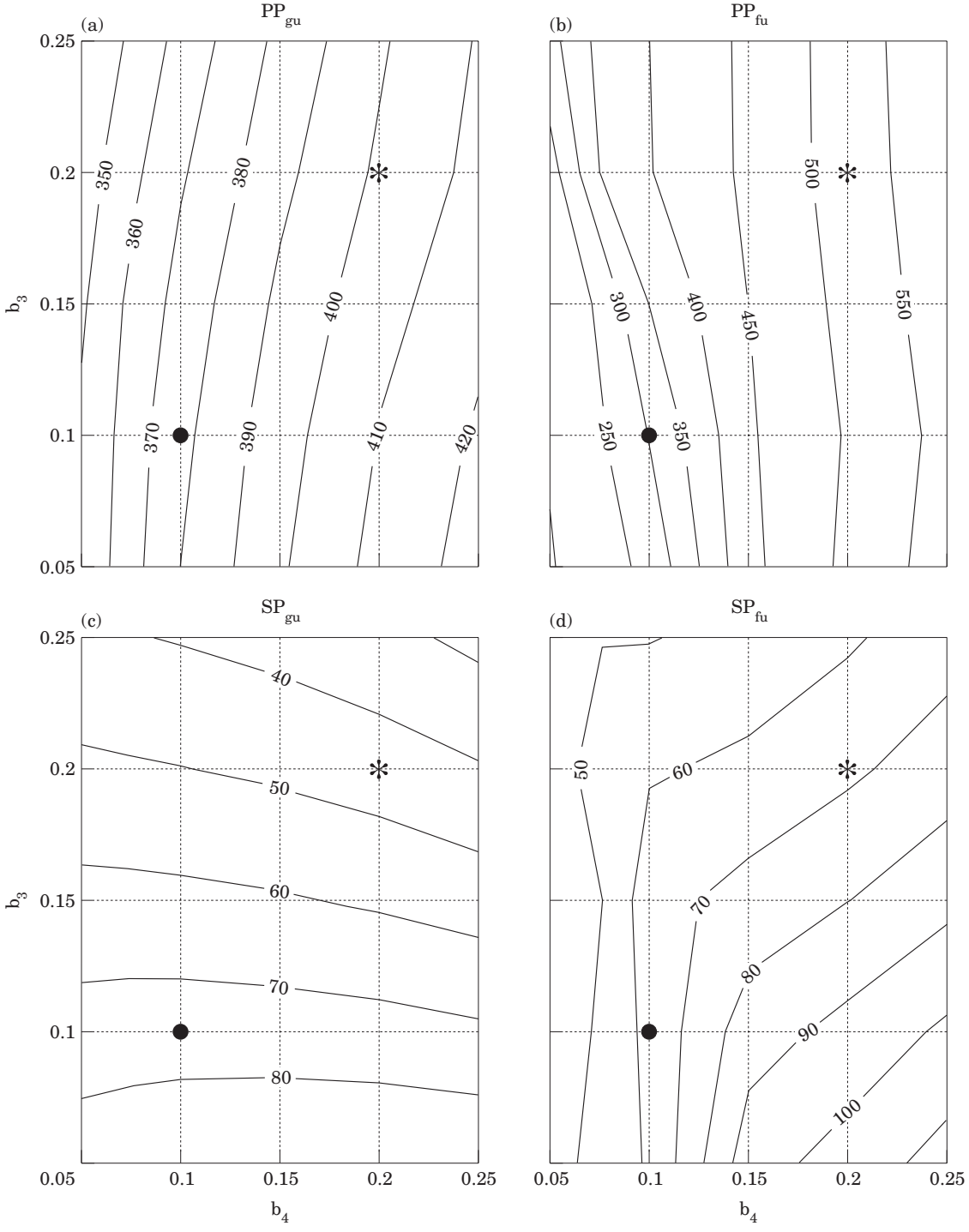

FIGURE 14. Sensitivity of the ecosystem to plankton mortality parameters b_3 and b_4. Contours of primary productivity in (a) the Strait of Georgia and in (b) Juan de Fuca Strait. Contours of secondary productivity in (c) the Strait of Georgia and in (d) Juan de Fuca Strait. All variables are in units of g Cm^{-2} $year^{-1}$. Symbol (●) corresponds to Run 1 and (*) to Run 3 in Figure 15(e).

hand, increasing phytoplankton mortality rates reduces the transfer of phytoplankton biomass to the higher trophic level and thus leads to smaller secondary productivity. As shown in Figure 15, the plankton stocks $Max(P_{gu})$ and $Mean(Z_{gu})$ in the Strait of Georgia generally decrease when either mortality rate

increases. The zooplankton population $Mean(Z_{fu})$ in Juan de Fuca Strait shows a similar trend, but the peak phytoplankton population $Max(P_{fu})$ increases with increasing zooplankton mortality b_4, similar only to the bottom left corner of Figure 15(a). Because the phytoplankton and zooplankton populations are closely coupled in Juan de Fuca Strait throughout the year, a decreasing zooplankton population is accompanied by increasing phytoplankton bloom size. In the contour diagram of ΔP_{max} [Figure 15(e)], there are again two regimes. There is a larger spring phytoplankton bloom in the Strait of Georgia in the shaded region.

Plankton mortality rats are not well known and difficult to measure, so the above sensitivity studies show only the range of behaviours that might be expected in the planktonic ecosystem. To examine this effect in further detail, we look at an example of plankton cycles labelled as Run 3 in Figure 15(e) with high mortality for both phytoplankton and zooplankton (see Table 1). As seen in Figure 16, the spring blooms occur later than in either Figure 4 or Figure 13. More significantly, the zooplankton in the Strait of Georgia remains low until later in the fall. This example illustrates another regime of the planktonic ecosystem, Regime 3, in which strong predation on the zooplankton (i.e. top-down control by an unspecified predator) causes a dramatic change in the plankton ecosystem in the Georgia–Fuca Estuary.

Regime 1 and 3 as predicted in the model appear to resemble observations of phytoplankton and zooplankton stock fluctuations in the Strait of Georgia during the two years in the mid-seventies (Stockner *et al.*, 1979). As shown in Figure 17, in year 1975 both phytoplankton and zooplankton are strongly peaked during the spring bloom (similar to Run 1 in Regime 1), while in year 1976 there was a large phytoplankton bloom but zooplankton stayed at low levels throughout the year (similar to Run 3 in Regime 3). Unfortunately, there are no corresponding observations in Juan de Fuca Strait. However, Figure 6 shows that chlorophyll *a* concentration in Juan de Fuca Strait can vary between 2 and 20 mg m^{-3} during spring blooms. The high chlorophyll *a* events are associated with significant drawdowns in the nitrate concentration. This suggests that significant spring blooms can develop in Juan de Fuca Strait, consistent with model results shown in Run 2 (Figure 13) and Run 3 (Figure 16).

Conclusion

In this paper a coupled biological–physical box model has been developed to investigate the seasonal and interannual variability of the planktonic ecosystem in a strongly estuarine system, the Strait of Georgia/Juan de Fuca Strait system on the west coast of Canada. The estuarine circulation redistributes plankton biomass within the system, causing an asymmetrical distribution of plankton biomass between the inner (Strait of Georgia) and outer (Juan de Fuca Strait) estuary. There appear to be three distinctive regimes of ecosystem behaviour: Regime 1 is characterized by a larger spring phytoplankton bloom in the Strait of Georgia; Regime 2 by a larger spring bloom in Juan de Fuca Strait; Regime 3 has the general characteristics of Regime 2, but with a low zooplankton population in the Strait of Georgia.

To consider the possible effect of interannual variability of the estuarine circulation, simulations have been performed with the coupled biophysical model under stochastic forcing in Fraser River runoff and in shelf salinity. It was found that the plankton populations are relatively insensitive to interannual changes in the estuarine circulation. However, the plankton populations appear to be sensitive to changes in biological rate parameters. Hence, change in the physical environment itself will dramatically affect the planktonic ecosystem only if it produces changes in these rate parameters. We thus suggest that interannual and interdecadal variability of the planktonic ecosystem might be associated with changes in the biological rate processes of marine phytoplankton and zooplankton. For example, a reduction in the zooplankton growth rate (grazing rate) might cause the planktonic ecosystem to switch from Regime 1 to Regime 2. An increase in the zooplankton mortality rate might move the planktonic ecosystem into Regime 3. However, it should be emphasized that these are only model simulations and existing observations are sparse.

The NPZ model used here is a simplified ecosystem model: it is possible that some of the model predictions may change when a more comprehensive ecosystem model is used. It would be more realistic if other factors are included in future ecosystem models. For example, we may consider the life history of the dominant zooplankton species *Neocalanus plumchrus*. A density-independent zooplankton mortality rate has been used in this study. Steele and Henderson (1992) and Fasham (1995) suggested that density-dependent mortality rate may be a better parameterization for the predation of zooplankton by (unresolved) higher trophic level predators. Future model improvements ought to explore this difference. Nevertheless, our work coupling a simple ecosystem model with an estuarine flow box model is a necessary step towards embedding more complex foodweb

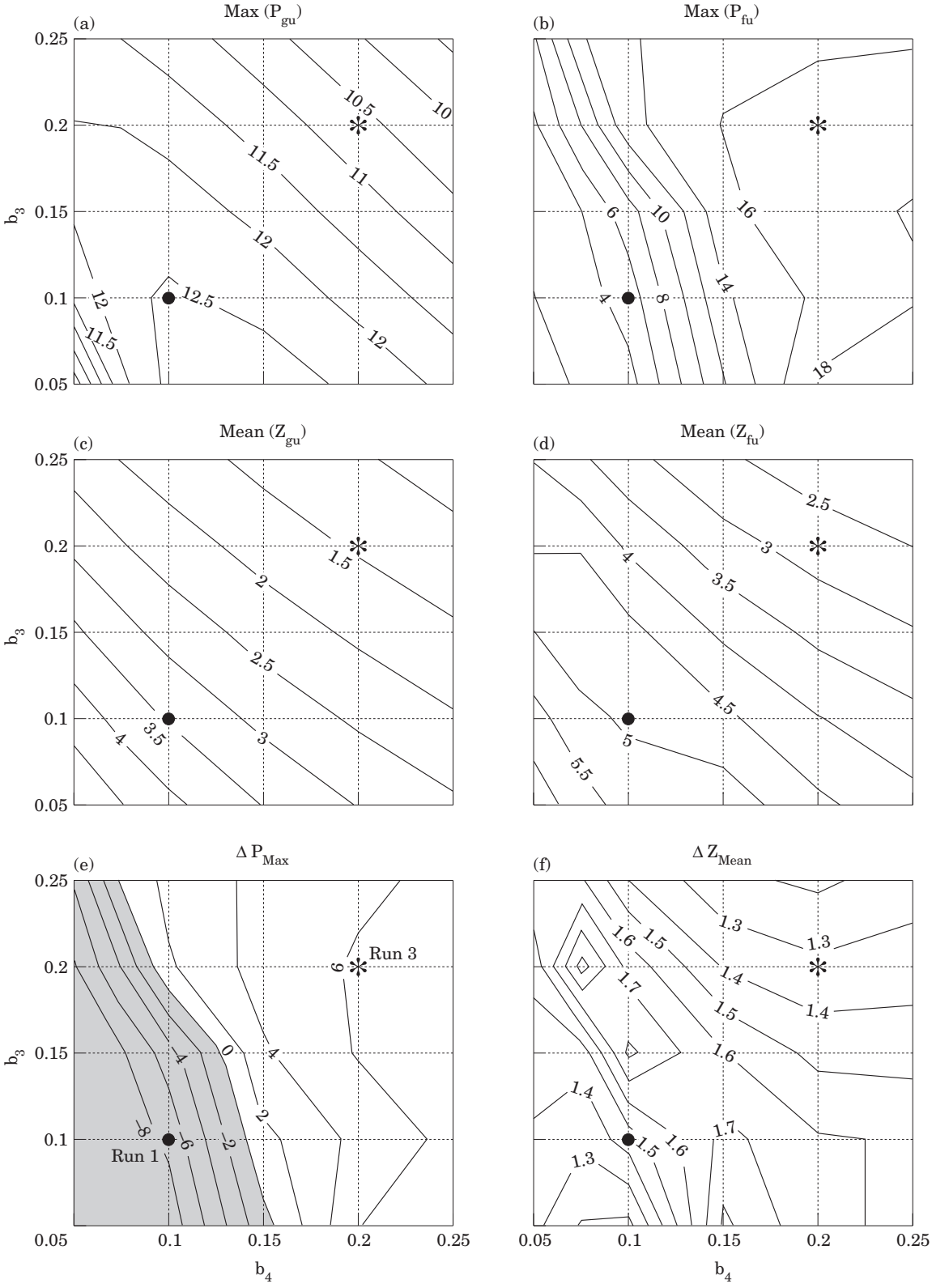

FIGURE 15. Sensitivity of the ecosystem behaviour to plankton mortality parameters b_3 and b_4. Contours of peak phytoplankton populations in (a) the Strait of Georgia and in (b) Juan de Fuca Strait. Contours of annually-averaged zooplankton populations (c) the Strait of Georgia and in (d) Juan de Fuca Strait. Contours of (e) ΔP_{max} and (f) ΔZ_{mean}. Point Run 1 (●) corresponds to the model run presented in Figure 4 and point Run 3 (*) to that in Figure 16. All variables are in units of mmol Nm^{-3}.

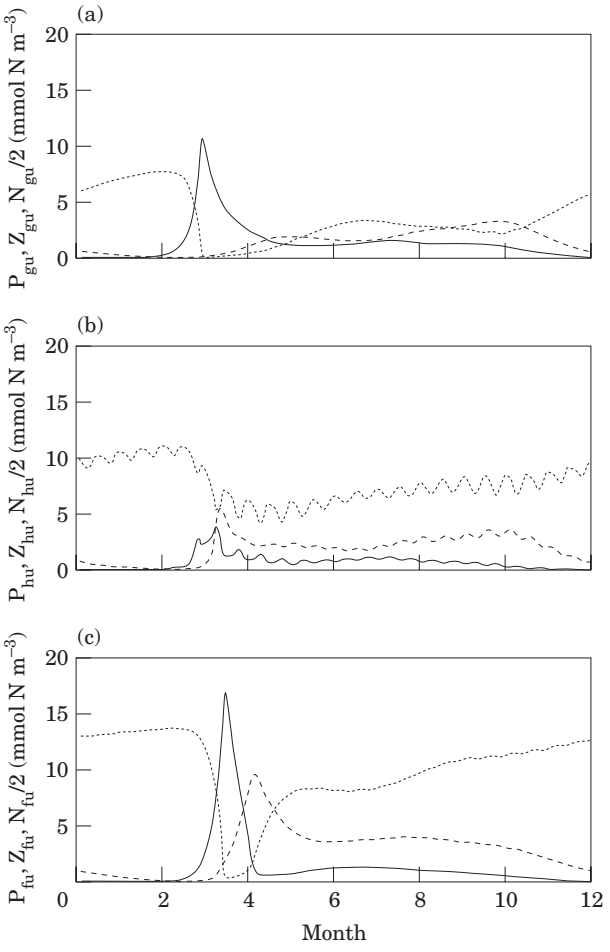

FIGURE 16. Seasonal variation of phytoplankton (solid), zooplankton (dashed) populations and nutrient concentration (dotted) in (a) the Strait of Georgia, (b) Haro Strait and (c) Juan de Fuca Strait [corresponds to Run 3 in Figure 15(e)].

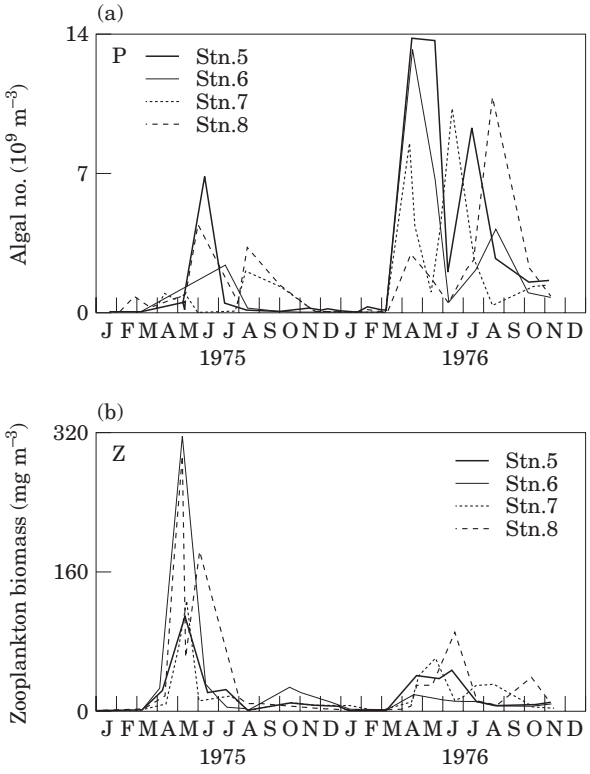

FIGURE 17. Phytoplankton concentrations and zooplankton biomass measured monthly at stations in the Strait of Georgia over a 2-year period (reproduced from Stockner *et al.*, 1979). Year 1975 resembles Run 1 shown in Figure 4 and year 1976 Run 3 shown in Figure 16.

models into increasingly complex estuarine flow models.

The ultimate test of any model prediction will be the comparison with actual observations of relevant marine ecosystems. There is a great need to maintain regular and intensive biological sampling programmes. Because phytoplankton blooms may occur within a short period of time (e.g. one month), a change in timing of the bloom or sampling by a week may produce dramatically different observations. Samplings at monthly intervals may thus miss important plankton dynamics and we should be cautious when comparing model results with such observations. This model suggests that the planktonic ecosystem in the Georgia–Fuca Estuary is sensitive to biological rate parameters and it might respond to climate variability through changes in these parameters. For example, an increase in the average sea temperature in the estuary may result in a faster phytoplankton growth rate. Future observations should be extended to include measurements of biological rate parameters.

The NPZ model results have shown that interannual variability of estuarine circulation only has a small effect on plankton productivity. Large fluctuations of some fish stocks observed in the Strait of Georgia may not be directly related to a rise or decline in the overall plankton productivity. For example, declines in Coho and Chinook salmon in recent years seem to be accompanied by large increases in herring and hake stocks (Dick Beamish (1998) pers. comm.). To relate fish stock fluctuations to climate variability, we may have to consider possible climatic impact on plankton community structure and develop structured foodweb models that can differentiate phytoplantkon and zooplankton species.

Acknowledgements

We are grateful to Dave Mackas, Dick Beamish and Paul Harrison for interesting discussions. We also

thank the referee for many helpful comments. Robin Brown's help with IOS database is greatly appreciated. This work was supported under Canadian Department of Fisheries and Oceans High Priority Project funding.

References

Beamish, R. J., Neville, C. M. & Cass, A. J. 1997 Production of Fraser River sockeye salmon (oncorhynchus nerka) in relation to decadal-scale changes in the climate and the ocean. *Canadian Journal of Fisheries and Aquatic Sciences* **54,** 543–554.

Beamish, R. J., Riddell, B. E., Neville, C. M., Thomson, B. L. & Zhang, Z. 1995 Declines in chinook salmon catches in the Strait of Georgia in relation to shifts in the marine environment. *Fisheries Oceanography* **4,** 243–256.

Beamish, R. J. & Bouillon, D. R. 1993 Pacific salmon production trends in relation to climate. *Canadian Journal of Fisheries and Aquatic Sciences* **50,** 1002–1016.

Cayan, D. R. & Peterson, D. H. 1989 The influence of North Pacific atmospheric circulation on stream flow in the west. In *Aspects of Climate Variability in the Pacific and the Western Americas* (Peterson, D. H., ed.). Geophysical Monograph, American Geophysical Union, Washington, D.C., pp. 375–397.

Chester, A. J., Damkaer, D. M., Dey, D. B. & Larrance, J. D. 1977 Seasonal distributions of plankton in the strait of Juan De Fuca. *NOAA Technical Memorandum* ERL MESA-24, pp. 1–70.

Denman, K. L., Mackas, D. L., Freeland, H. J., Austin, M. J. & Hill, S. H. 1981 Persistent upwelling and mesoscale zones of high productivity off the west coast of Vancouver Island, Canada. In *Coastal Upwelling* (Richards, F. A., ed.). American Geophysical Union, pp. 514–521.

Ebbesmeyer, C. C., Coomes, C. A., Cannon, G. A. & Bretschneider, D. E. 1989 Linkage of ocean and fjord dynamics at decadal period. In *Aspects of Climate Variability in the Pacific and the Western Americas* (Peterson, D. H., ed.). Geophysical Monograph, American Geophysical Union, Washington, DC, pp. 399–417.

Evans, G. T. & Parslow, J. S. 1985 A model of annual plankton cycles. *Biological Oceanography* **3,** 327–347.

Fasham, M. J. R., Ducklow, H. W. & McKelvie, S. M. 1990 A nitrogen-based model of plankton dynamics in the ocean mixed layer. *Journal of Marine Research* **48,** 591–639.

Fasham, M. J. R. 1995 Variations in the seasonal cycle of biological production in subarctic oceans: A model sensitivity analysis. *Deep-Sea Research* **42,** 1111–1149.

Frost, B. W. 1993 A modelling study of processes regulating plankton standing stock and production in the open subarctic Pacific. *Progress in Oceanography* **32,** 17–57.

Gargett, A. E. 1997 The optimal stability ' window ': a mechanism underlying decadal fluctuations in North Pacific salmon stocks? *Fisheries Oceanography* **6,** 109–117.

Harrison, P. J., Futton, J. D., Taylor, F. J. R. & Parsons, T. R. 1983 Review of the biological oceanography of the Strait of Georgia: Pelagic environment. *Canadian Journal of Fisheries and Aquatic Sciences* **40,** 1064–1094.

Healey, M. C. 1980 The ecology of juvenile salmon in Georgia Strait, British Columbia. In *Salmonid Ecosystem of the North Pacific* (McNeil, W. J. & Hinsworth, D. C., eds). Oregon State University Press, Corvallis, pp. 203–229.

Hill, S., Derman, K., Mackas, D. & Sefton, H. 1982. Ocean ecology data report: coastal waters off southwest Vancouver Island. Spring and Summer 1980. *Canadian Data Report of Hydrography and Ocean Science No. 4.* 103 pp.

Li, M., Gargett, A. E. & Denman, K. L. 1999 Seasonal and interannual variability of estuarine circulation in a box model of the Strait of Georgia and Juan de Fuca Strait. *Atmosphere-Ocean* **37,** 1–19.

Mackas, D. L. & Harrison, P. J. 1997 Nitrogenous nutrient sources and sinks in the Juan de Fuca Strait/Strait of Georgia/ Puget Sound estuarine system: Assessing the potential for eutrophication. *Estuarine, Coastal and Shelf Science* **44,** 1–21.

Pickard, G. L. & Emery, W. J. 1990 *Descriptive Physical Oceanography: An Introduction*. Pergamon Press, 320 pp.

Steele, J. H. & Henderson, E. W. 1992 The role of predation in plankton models. *Journal of Plankton Research* **14,** 157–172.

Stockner, J. G., Cliff, D. D. & Shortreed, K. R. S. 1979 Phytoplankton ecology of the Strait of Georgia, British Columbia. *Journal of the Fisheries Research Board of Canada* **36,** 657–666.

Stommel, H. 1961 Thermohaline convection with stable regimes of flow. *Tellus* **13,** 224–230.

Sverdrup, H. U. 1953 On conditions for vernal blooming of phytoplankton. *J Cons Perm Int Explor Mer* **18,** 287–295.

Thomson, R. E. 1994 Physical oceanography of the Strait of Georgia–Puget Sound–Juan de Fuca Strait system. In *Review of the Marine Environment and Biota of Strait of Georgia, Puget Sound and Juan de Fuca Strait: Proceedings of the BC/Washington Symposium on the Marine Environment* (Wilson, R. C. H., Beamish, R. J., Aitkens, F. & Bell, J., eds). pp 39–98.

Thomson, R. E. 1981 Oceanography of the British Columbia coast. *Canadian Special Publication of Fisheries and Aquatic Sciences* **56,** 291.

Appendix

Li *et al.* (1999) developed a six-box model of estuarine circulation for the Strait of Georgia and Juan de Fuca Strait (see Figure 2). The estuary is divided into Georgia, Haro and Fuca basins (denoted by g, h and f), each of which has volume V, horizontal area A and consists of an upper and lower box (denoted by u and l). The upper box has a depth of h_u=50 m while the lower box has a depth of h_l=150 m.

The estuarine circulation is driven by the Fraser River runoff Q_r. Fresh water dilutes the upper layer of the Strait of Georgia and the resulting density difference between the Strait of Georgia and Haro Strait drives a two-layer circulation between the two straits: fresher water exported to Haro Strait in the surface layer and saltier water imported to the Strait of Georgia in the lower layer. The circulation is closed by an upwelling branch in the Strait of Georgia and a downwelling branch in Haro Strait. Similarly, the density contrast between Haro Strait water and Juan de Fuca Strait water drives a second circulation between those two straits. Because the west end of Juan de Fuca Strait is open to the Pacific Ocean, fresher water is exported to the Pacific at the surface and saltier water imported from the Pacific at depth. This estuarine circulation is modulated by tidal mixing, particularly in tidally-energetic Haro Strait, as shown by two-way arrows in Figure 2. Weaker vertical mixing occurs in the Strait of Georgia and Juan de Fuca Strait.

The water mass transport between the basins is parameterized using Stommel's formula (Stommel,

1961). If Q_g is the volume flux between the Georgia and Haro basins and Q_f is that between the Haro and Fuca basins, then $Q_g = c_g\beta\rho_0(S_{hu} - S_{gu})$ and $Q_f = c_f\beta\rho_0(S_{fu} - S_{hu})$ where c_g and c_f are two proportional constants, β the saline contraction coefficient, ρ_0 a reference density and S the salinity. Tidal mixing in Haro Strait has a spring-neap cycle but its magnitude is reduced when stratification in the strait exceeds a threshold ΔS_c. The mixing coefficient in Haro Strait is given by $\omega_h = \frac{1}{2}\omega_h^m\left(1 + \sin\frac{2\pi t}{T/24}\right) f(S_{hl} - S_{hu})$ in which ω_h^m is the maximum value, T the length of a year and $f = \Delta S_c/(S_{hl} - S_{hu}) > 1$ when the stratification $(S_{hl} - S_{hu}) > \Delta S_c$. The two-layer exchange flow between Juan de Fuca Strait and the Pacific Ocean is represented by horizontal advection terms in the salinity equations. In addition, the deep salinity of Juan de Fuca Strait is relaxed to that of the Pacific Ocean with a time scale t_r.

The governing equations for the salinities in each box are given by:

$$V_{gu}\frac{dS_{gu}}{dt} = Q_g(S_{gl} - S_{gu}) + \omega_g A_g(S_{gl} - S_{gu}) - Q_r S_0, \quad (22)$$

$$V_{gl}\frac{dS_{gl}}{dt} = Q_g(S_{hl} - S_{gl}) - \omega_g A_g(S_{gl} - S_{gu}), \quad (23)$$

$$V_{gl}\frac{dS_{gl}}{dt} = Q_g(S_{hl} - S_{gl}) - \omega_g A_g(S_{gl} - S_{gu}), \quad (23)$$

$$V_{hl}\frac{dS_{hl}}{dt} = Q_g(S_{hu} - S_{hl}) + Q_f(S_{fl} - S_{hl}) - \omega_h A_h(S_{hl} - S_{hu}), \quad (25)$$

$$V_{fu}\frac{dS_{fu}}{dt} = Q_f(S_{hu} - S_{fu}) + \omega_f A_f(S_{fl} - S_{fu}), \quad (26)$$

$$V_{fl}\frac{dS_{fl}}{dt} = Q_f(S_{fu} - S_{fl}) - \omega_f A_f(S_{fl} - S_{fu}) + \frac{1}{t_r}V_{fl}(S_p - S_{fl}). \quad (27)$$

These equations can be nondimensionalized to reduce the number of parameters. There are six dimensionless parameters which control the dynamics of the estuarine circulation:

$$F_1(t) = R_{1w} + R_1 sech^2\left[10\frac{(t - T/2)}{T}\right],$$

$$R_{1w} = \frac{Q_{rw}}{c_g\rho_0\beta S_0}, \qquad R_1 = \frac{Q_{rs}}{c_g\rho_0\beta S_0}, \quad (28)$$

$$R_2 = \frac{\omega_g A_g}{c_g\rho_0\beta S_0}, \quad (29)$$

$$R_3 = \frac{c_f}{c_g}, \quad (30)$$

$$R_4 = \frac{\omega_h A_h}{c_g\rho_0\beta S_0} = \frac{1}{2}R_4^m f(S_{hl} - S_{hu})\left(1 + \sin\frac{2\pi t}{T/24}\right),$$

$$R_4^m = \frac{\omega_h^m A_h}{c_g\rho_0\beta S_0}, \quad (31)$$

$$R_5 = \frac{\omega_f A_f}{c_g\rho_0\beta S_0}, \quad (32)$$

$$R_6 = t_s/t_r. \quad (33)$$

The coefficient in the Stommel's parameterization is an adjustable parameter. Li *et al.* (1999) chose $c_g\rho_0\beta S_0 = 10^6\ m^3\ s^{-1}$ to produce a realistic seasonal cycle of salinities. F_1 is the ratio of the freshwater flux to this water volume transport rate. To simulate pronounced peak discharge in summer, we use a hyperbolic function to describe the seasonal variation of the river runoff. The winter runoff $Q_{rw} \approx 10^3\ m^2\ m^{-3}$. The peak summer runoff, Q_{rs} is about 10 times larger and varies from year to year (Thomson, 1994). $R_3 = c_f/c_g$ is a ratio of two proportional constants and is assumed to be 1. The other three parameters R_2, R_4 and R_5 are ratios of rates of water mass exchange due to vertical mixing to the water mass transport due to density differences. ω_g and ω_f are constant mixing coefficients in the Georgia and Fuca basins. We chose $\kappa_v = 1{\cdot}25 \times 10^{-4}\ m^2\ s^{-3}$ for the Strait of Georgia and $\kappa_v = 1{\cdot}25 \times 10^{-3}\ m^2\ s^{-3}$ for Juan de Fuca Strait. For Haro Strait, we chose $R_4^m = 0{\cdot}5 (\kappa_v = 5 \times 10^{-2}\ m^2\ s^{-3})$ and a threshold stratification $\Delta\tilde{S}_c = 0{\cdot}2$ above which mixing is progressively suppressed. The model results are not sensitive to changes in these parameters within reasonable ranges. The nondimensional time scale $t_s = V_{gu}/(c_g\rho_0\beta S_0) = 2 \times 10^5\ s \approx 2{\cdot}3$ day. The last parameter R_6 is the ratio of t_s to t_r, the time for the deep water salinity of Juan de Fuca Strait to relax to a prescribed boundary salinity. Li *et al.* (1999) found that $(3t_r) = 2$ months gives a good fit for the seasonal cycle of salinities in Juan de Fuca Strait, although the model results are relatively insensitive to t_r for $(3t_r)$ ranging from one to six months.

Figure 3(a) shows the seasonal cycle of salinities in the six boxes. The Fraser River freshet in early summer significantly dilutes the salinity in the upper box of the Strait of Georgia. The fresh water is exported first to Haro Strait and then to Juan de Fuca Strait. Reduced mixing in Haro Strait leads to a

summer stratification much stronger than that in the winter. Late-summer upwelling over the shelf produces high salinity in the deep box of Juan de Fuca Strait. This high salinity water is transported into the other two straits, restoring the salinities back to the winter levels. Figure 3(c) shows the volume fluxes, Q_g between the Georgia and Haro basins, and Q_f between the Haro and Fuca basins. They are typically an order of magnitude larger than the river runoff. These model predictions are in agreement with observations (cf. Li *et al.*, 1999).